8

Preparation of Selected Ceramic Compounds by Controlled Crystallization Under Hydrothermal Conditions

Juan Carlos Rendón-Angeles[1], Zully Matamoros-Veloza[2] and Kazumichi Yanagisawa[3]
[1]*Research Institute for Advanced Studies of the NPI Saltillo Campus*
[2]*Technological Institute of Saltillo*
[3]*Research Laboratory for Hydrothermal Chemistry, Kochi University*
[1,2]*México*
[3]*Japan*

1. Introduction

The main aim of this chapter is to review some particular aspects related with the hydrothermal crystallization process for preparing some selected oxide and non-oxide powders, namely functional compound with electric, piezoelectric, ionic conducting and catalytic properties. The literature on the hydrothermal crystallization of oxide and non-oxide powders is vast; the references cited here are those more appropriated to illustrate this review. A particular attempt is made to broaden the traditional concepts of processing perovskite powders with controlled chemical composition and particle morphology, those aspects will be discussed based on the chemical reactivity of the precursor reactants (gels). Furthermore, an additional approach that takes into account the solubility of the solid species (mineral reagents) that are employed as a precursor in the hydrothermal systems on controlling the crystallization process of oxide particles was further investigated for preparing titanates oxide ceramic. The specific reaction pathways and kinetic aspects are discussed and illustrated by experimental setups for the solution of selected problems in hydrothermal crystallization. Also the chapter includes recent work on the formation of inorganic salts of Sr or Ba, under ordinary hydrothermal treatments via the anionic replacement in sulphate minerals, because these particular reactions have promoted peculiar microstructure on the crystallized material that preserves the bulk geometrical features of particular mineral specie. Therefore, this method could be attractive for preparing net-shaped materials with controlled porosity, with optimized functional properties, because can be used as gas sensor, substrates for porous catalytic materials, filters, among other potential applications.

2. Hydrothermal crystallization as technique for oxide and non-oxide synthesis

2.1 Brief history of the hydrothermal technique development

The studies recorded at the scientific annals indicate that the pioneering research on hydrothermal systems was initiated in the middle of the 19th century (Schafthaul, 1845, as

cited in Suchanek et. al., 2004). The term of hydrothermal is purely of geological origin; this was firstly used by the geologist Sir Roderick Murchinson (1792–1871), whom analysed the reactivity of water at elevated pressure and temperature, to explain the mineral formation of several rocks and minerals (Byrappa & Yoshimura, 2001). Continuous progress in material synthesis was initially accelerated by notorious developments in hydrothermal pressure vessels apparatus. Hence, at the first decade of the 20th century, geologist achieved a marked technological expansion on the hydrothermal research field, namely efforts were directed towards for designing the first metal vessels and carried out preliminary experiments at laboratory scale related to material synthesis area, mainly in the field of inorganic single crystal growth (Riman et. al., 2002; Suchanek et. al., 2004). However, the development of chemical reactions via hydrothermal processing was further limited because of the severe treatment (supercritical) conditions, which were normally required for single crystal growth. This resulted on discourage extensive research and commercialization of various materials. Hydrothermal epitaxial growth is one example, it was popular during the 1970s, but it did not reach commercial success due to the high temperatures (> 500 °C) and pressures (> 100 MPa), which were involved to achieve the epitaxial crystal growth process. In the middle of the 1980s, the commercial interest in the hydrothermal technology was revived, because the steadily increasing of a large group of materials, manly ceramic powder, had emerged that can be produced under more environmentally friendly conditions (T < 350 °C, P < 100 MPa). At present, the major developments on the hydrothermal synthesis technology including in particular the hydrothermal crystallization has been accomplished in several countries around the world like: China, Japan, USA, UK, Germany and some others with minor contributions (Byrappa & Yoshimura, 2001).

2.2 Definition of hydrothermal synthesis

The term "*hydrothermal*" is difficult to define, based in the etymologic root of the Greek word, "*hydrous*" means water and "*thermal*" means heat. One of the accepted statements for hydrothermal defines it as any heterogeneous chemical reaction that occurs in the presence of a solvent media at above the room temperature (> 25 °C) and pressure levels greater than 0.1 MPa in a closed system, at these conditions does not matter whether the solvent is aqueous or non-aqueous. Hitherto, there is still a bit of confusion regarding the correct use of the term hydrothermal, because in the case of the chemistry field, the chemists prefer to use a different term, namely *solvothermal*, which means any chemical reaction conducted with a non-aqueous solvent or solvent in supercritical conditions. Additionally, another similar related terms widely used amongst the physicist, chemist and material scientist communities are: *glycothermal*, *alcothermal*, *ammonothermal*, and so on. However, some researchers also use hydrothermal for describing processes conducted at ambient conditions. The *crystallization* process of solid phases under hydrothermal conditions is usually conducted at autogeneous pressure, achieving a particular saturated vapour pressure of the solution at the specified temperature and composition of the hydrothermal solution. In this concern, in terms of industrial commercial processes mild operating conditions are preferred, for example treatment temperatures below than 350 °C and pressures > 50 MPa (Byrappa, 2005). The limit that indicates the transition from mild to severe conditions during a hydrothermal treatment is normally determined by the strength of the inner vessel materials, which at severe treatment conditions undergoes into a corrosion process. The continuous research in this field has led the way to a better understanding for controlling chemical reactions in various hydrothermal medias, which

has remarkably reduced the processing parameters such as: reaction time, temperature, and pressure for hydrothermal crystallization of several oxide and non-oxide materials (T<200 ^{o}C, P<1.5 MPa). At present, the recent scientific and technological achievements have made hydrothermal synthesis more economical, because powder preparation can be carried out by a single step cost-effective process, in advanced pressure reactor technology coupled with processing methodologies proposed for a wide number of inorganic compounds (Suchanek et al., 2004).

2.3 Hydrothermal processes for synthesis of inorganic compounds

2.3.1 Hydrothermal single crystal growth

Regardless of the numerous investigations on hydrothermal single crystal growth, quartz crystal is one of the materials extensively investigated up to now. Nowadays, the electronic industry requires the use of pure large single crystals of synthetic origin, because natural quartz crystals are generally irregular in shape, and is difficult to obtain large-scale single crystals wafers by automatic cutting. The crystal growth of oxide species, namely α-quartz; is conducted by the conventional hydrothermal temperature gradient method, thus, the autoclaves frequently used consist of two chambers were different process occurs. One of the important parameter to consider for the single crystal growth of α–quartz is the selection of the proper nutrient material; among the most employed are small particle size α–quartz, silica glass, high quality silica sand, or silica gel (Byrappa 2005). The nutrient reactant is placed at the liner chamber (vessel bottom, see Figure 1) made up of iron, silver or titanium that is less employed, with a suitable baffle and a frame (at the top of the vessel) holding the seed of the material that is been grown. The mineralizer solution is other factor to select coupled with a definite molarity; this is poured into the liner to make the required filling volume and achieves the dissolution of the nutrient. Under these conditions, matter transport proceeds from the nutrient chamber and the crystallization and growth of the crystals is achieved due to the temperature difference at the top-seeded part of the autoclave. The particular optimum conditions determined at Bell Laboratories for growing quartz single crystals are dissolution temperature of 425 ^{o}C at a pressure in the range of 100–175 MPa, the crystallization and simultaneous growth proceeds at 375 ^{o}C whilst the temperature gradient from the nutrient to the growing chamber was of 50 ^{o}C. The mineralizer employed was an alkaline solution of NaOH with concentration varying between 0.5 up to 1 M, and the volume of poured mineralizer solution varied in the range of 78–85 % of the total volume of the vessel (Laudies, 1970; as cited in Byrappa, 2005).

The crystallization and growth of other single crystals rather than SiO_2 was firstly investigated for oxide species, namely TiO_2, ZrO_2, HfO_2 and some related perovskite oxides $PbTiO_3$ and $PbZrO_3$. Experimental results evidenced that the mineralizer employed for dissolving and transport the nutrient reactant markedly affected the crystallization of the oxides and the crystal growth. Thus, the single oxide species were found to dissolve and recrystallize faster in fluoride solutions (NaF, KF and NH_4F) in comparison with alkalis, KOH and K_2CO_3, because of the high chemical reactivity of these nutrient oxides in fluoride solutions. However, the complete dissolution and transport of the nutrient was preferentially achieved in NH_4F solutions rather than NaF or KF mineralizers, even at a low temperature of 470 ^{o}C for a reaction interval up to 6 days (Kuznetzov, 1968), and the TiO_2, ZrO_2, HfO_2 single crystal growth was achieved at a temperature of 520 ^{o}C with a positive temperature gradient

(30 °C). This is a popular method that promotes the crystal growth and has been widely used on the preparation of berlinite ($AlPO_4$) crystals (Byrappa & Yoshimura 2001).

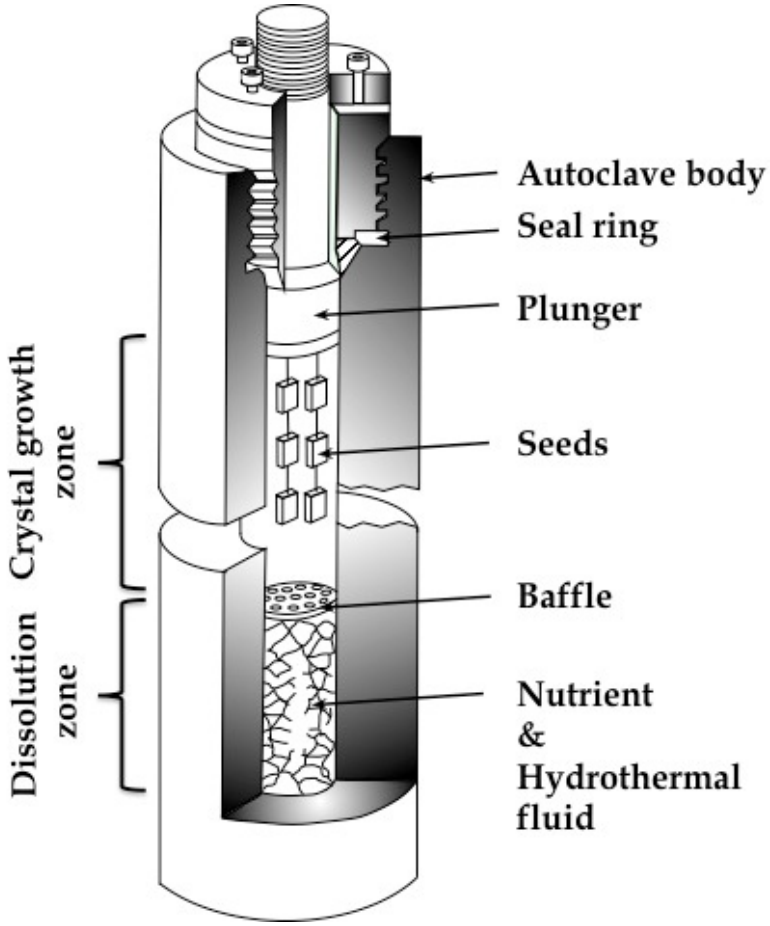

Fig. 1. Scheme of the conventional autoclave employed for single crystal growth under hydrothermal conditions (Schubert, 2000; as cited in Byrappa & Yoshimura, 2001).

A particular emphasize on the hydrothermal crystal growth research has been focused for the crystallization of materials that melts incongruently because such materials cannot be grown with compositional and phase uniformity. The relevant examples of compounds that melts incongruently are those belonging to lead family oxides titanate ($PbTiO_3$), zirconate ($PbZrO_3$), single crystals with millimetre size of both compounds were found to grown satisfactorily in NH_4F hydrothermal solution by seedless grown crystallizing conditions at temperatures between 500–600 °C for several days (Kuznetzov, 1968). However, the hydrothermal crystal grown of some lead related solid solutions, $PbZr_{1-x}Ti_xO_3$ (PZT), $PbMg_{1/3}Nb_{2/3}O_3$ (PMN) and $PbSc_{0.5}Nb_{0.5}O_3$ (PSN), is limited due to the low chemical stability of the perovskite structure even in KF solution, and results on the grown of small

single crystals with pyrochlore structure $Pb_{1.83}Mg_{0.29}Nb_{1.71}O_{6.39}$ and $Pb_{1.83}Sc_{0.29}Nb_{1.71}O_{6.39}$, as shown in Figure 2 (Yanagisawa et. al., 1999, 2000). This incongruence has not been determined thermodynamically and experimentally for the PZT, because this compound has been used to grown thin and thick single crystals on different seeds ($SrTiO_3$) with excellent compositional control (Oledzka et. al., 2003). In general, the crystallization and crystal growth of a specific compound can be carried out using different mineralizer or solvents, e.g., water, soluble salts, acid solutions, non aqueous solutions; but some physicochemical factors must be taking into account to fulfil suitable conditions that facilitate both processes.

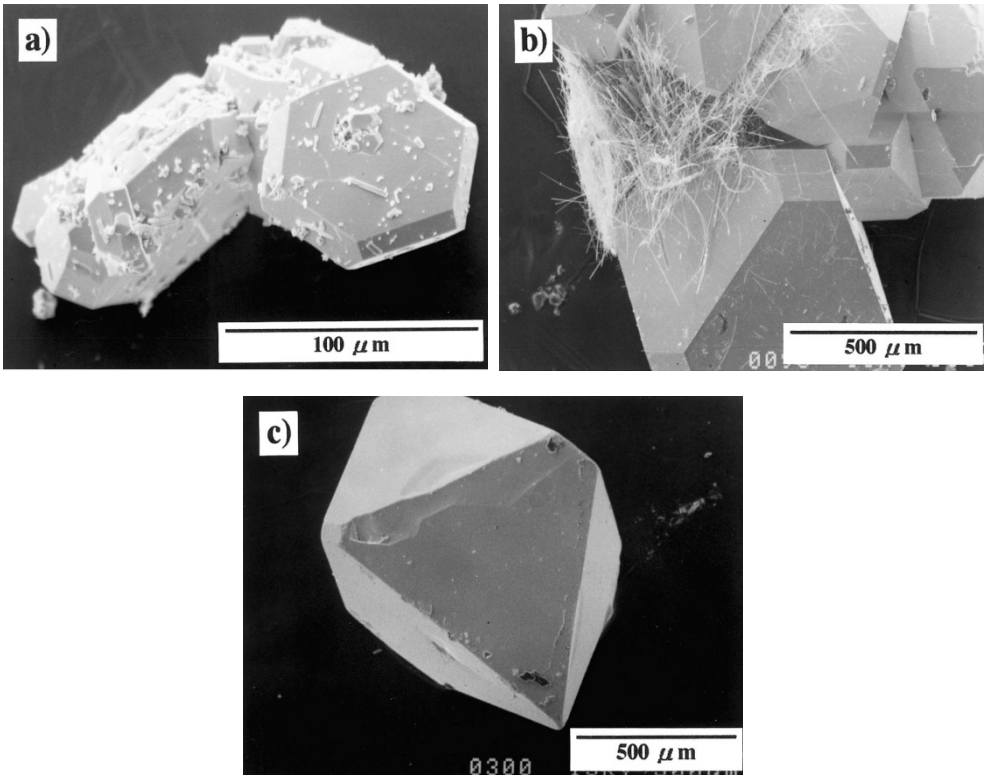

Fig. 2. Pyrochlore single crystals, of (a) PMN, (b) PSNT and (c) PSN; grown at the top of platinum capsule at 600 °C with a gradient temperature gradient of 40 °C in KF solutions 5, 4.2 and 6.2 M for reaction intervals of 3 (a) and 5 days (c,d), respectively (Yanagisawa et. al., 1999).

2.3.2 Advanced hydrothermal processing methods

Remarkable achievements for developing the *Hydrothermal Microwave Assisted Synthesis* process have been conducted at Pennsylvania State University (Komarneni et. al., 1992); this method enhances solid crystallization kinetics 1–4 order of magnitude faster than that occurring on the conventional hydrothermal processing for a wide solutions. In addition, other advantages of the hydrothermal microwave assisted technique are very high heating

rates and the synthesis of novel phases. A great variety of ceramic powders with particular morphologies and controlled particle size, have been produced, e.g. TiO_2, ZrO_2, Fe_2O_3, $BaTiO_3$, $Ca_{10}(PO_4)_6(OH)_2$, etc (Komarneni et. al., 1992; Roy, 1994; Komarneni et. al., 2002).

Another variation implemented to the hydrothermal conventional process resulted on the development of a different hybrid method denominated *Hydrothermal-Electrochemical Synthesis*. This technique was tailored to deposit polycrystalline oxide films on reactive metal substrates. This technique becomes very important when the crystallization of oxide products from supersaturated hydrothermal solutions is hinder in absence of an applied electrical potential. Nowadays, highly crystallized ceramic thin films, such as a $BaTiO_3$, $SrTiO_3$, $LiNiO_2$, $PbTiO_3$, $CaWO_4$ and $BaMoO_4$ can be deposited on metal substrates from aqueous solutions at relatively low temperature 50–200 ^oC for several hours under a continuous applied voltage charge (Yoshimura & Suchanek, 1997). Additionally, semiconductor thin layers of GaAs, CdTe, CdSe and CdS have been successfully prepared by electrochemical atomic layer epitaxy growth, this mechanism is analogous to molecular epitaxy, however, the crystallization and growth of the layer is enhanced from a saturated hydrothermal media instead of a vapour phase that transport the growing species (Colletti et. al., 1998; as cited in Suchanek et. al., 2004).

Among other tailored techniques, the high energy milling technique has been challenged to hybridize the conventional hydrothermal processing, resulting in a coupled process that involves the classical powder mechanochemical and hydrothermal syntheses. The *Mechanochemical-Hydrothermal* route utilizes the solvency of an aqueous solution, which facilities the crystallization of solid species due to the pressure environment generated inside the mechano-chemical autoclave; it mainly accelerates the rate-determining steps of those factors, for instance: interfacial reaction, solute dissolution or dehydroxylation; that limit hydrothermal chemical reactions at low temperature. These reactions enhance the crystallization to occur locally at the particle surface because of the perturbation of superficial bonded species in the solid coupled with high temperature gradients (400–700 ^oC) and pressure localized zones that are generated during the mechanical activation of slurries. This is mainly promoted by the friction and adiabatic heating of gas bubbles while maintaining the average temperature close to room temperature (Kosova et. al., 1997; as cited in Suchanek et. al., 2004). Hitherto, this technique has been used for preparing bioceramic materials such as hydroxyapatite (Suchanek et. al., 2002; Chen et. al., 2004), another tailored material like $PbTiO_3$ was also crystallized by this technique.

Since Rustum Roy reported that the use of ultrasonic devices are feasible for improving low temperature inorganic syntheses because reaction kinetics is two orders of magnitude faster than that for the conventional wet chemistry synthesis methods (Roy, 1994). Some attempts to adapt ultrasonic devices emitting acoustic signals of 20 kHz up to 10 MHz have been conducted, because the acoustic signal produce very sharp temperature gradients with localized peak temperature zones, speculated as high as 5000 K, as well as, localized pressure zones of up to 100's MPa. The sonochemical environment also alters the molecular chemistry (chemical bond scission, generate excited states and accelerate electron transfer steps in chemical reactions), and enhances mass transport and crystallization kinetics due to the high convection of the fluid. (Peters, 1996, as cited in Riman et. al., 2002). *Hydrothermal-sonochemical synthesis* method have been used for preparing various ceramic powders

($Ca_{10}(PO_4)_6(OH)_2$, $AlPO_4$, InSb, CdS) and thin films ($Li_2B_4O_7$, $Ba_2TiSi_2O_8$).while the average temperature of the reactors is maintained close to room temperature.

The advanced hydrothermal techniques discussed in this section, even though wet chemical synthesis is offer in conjunction with so many significant advantages over the conventional method, might be able to have wide application in the industry. Compared to solid-state materials processing, these technologies might be more facile for scaling up. This situation, however, still cannot guarantee successful application of all these technologies to industries. Hence, much effort is needed to obtain a more comprehensive understanding of several physicochemical phenomena related to each of the new technologies hybridizing the conventional hydrothermal synthesis, in order to establish a relationship between science and technology that could lead to optimize these methods for their employment at a industrial scale (Shi & Hwang, 2003).

2.4 Conventional hydrothermal crystallization process for advanced ceramic materials

2.4.1 Factors that affect optimizing hydrothermal crystallization experiments

In general, a majority of the hydrothermal synthesis research work that has been done in the past was based on Edisonian trial and error design for process development, but this is not the best experimental approach for discerning between processes that are controlled by either thermodynamics or kinetics. In contrast, much effort has been paid to use thermodynamic modelling for processing design; this approach is based on fundamental physicochemical principles instead of the Edisonian methods (Riman et. al., 2002). Therefore, a great number of hydrothermal fundamental works for some particular solid-aqueous systems have provided sufficient experimental hydrothermal physical chemistry data. An important point derived from these works is related with the behaviour of the solvent under hydrothermal conditions, because it has a relationship with aspects like structure at critical, supercritical and sub-critical conditions, solution dielectric constant, pH variation, viscosity, expansion coefficient, density, etc., all these parameters depend markedly on thermodynamic variables such as pressure and temperature. At present, hydrothermal crystallization process is the only one where a fundamental understanding of kinetics is lacking due to the absence of physicochemical data of the intermediate phases forming in specific aqueous solutions. Although, fundamental research works related to synthesis of specific compounds demonstrated the importance of crystallization kinetics, however, a better understanding of crystallization kinetics still in an early stage of development. In this case, due to the absence of predictive methodology models, ones must estimated on terms of chemical equilibrium of the reaction the effect of temperature, pressure, precursor, and time to achieve solid crystallization and improve the reaction kinetics. Insight into this would enable us to understand how to control the formation of ionic species in the solution, the crystallization of solid phases and the rate of their growth.

In the last decade, much effort has directed towards for developing thermochemical models based in fundamental knowledge of thermodynamic and the Hegelson-Kirkham-Flowers-Tanger equation of state, which allows to represent standard-state properties across substantial temperature and pressure ranges in order to estimate chemical reactions path ways under hydrothermal conditions (Lencka & Riman, 2002). Modelling can be

successfully applied to very complex aqueous electrolytes over specific ranges of temperature and reactant and solvent concentration and non-aqueous systems can also be model as well. Practical computer software for conducting thermochemical modelling studies was recently developed by OLI System Inc., USA. This software can be used to conduct studies for chemical reactions for hydrothermal systems within the temperature range of -50 to 300 ^{o}C, at pressures ranging from 0 to 150 MPa and concentration of 0 up to 30 m in molar ionic strength; for the non-aqueous systems the temperature range covered is from 0 to 1200 ^{o}C and pressure from 0 to 150 MPa with species concentration from 0 to 1.0 mole fraction. Major predictions using the thermodynamic model have been done to determine the optimum hydrothermal conditions for achieving the crystallization of a wide variety of oxides such as, $BaTiO_3$, $PbTiO_3$, $CaTiO_3$, $SrZrO_3$ and $(BaSr)TiO_3$ (Lencka & Riman, 1993, 1995; Gersten et. al., 2004).

Currently, the research efforts on the thermochemical-modelling topic are being focused to establish an overall rational engineering-based methodology that will speed up process development. The proposed methodology for conducting this study involves the following four steps:

1. Compute thermodynamic equilibrium as a function of chemical processing variables.
2. Generate equilibrium diagrams to draw the process variable space for the phases of interest.
3. Design hydrothermal experiments to test and validate the computed diagrams.
4. Utilize the processing variables to explore opportunities for controlling reactions and crystallization kinetics.

Recently, population balance modelling has received much attention from both academic and industrial areas because of its applicability to a wide variety of particular processes. In general, a population balance model can be proposed by the collective phenomenology contained in entities displacement through their state space and the birth-and-death processes that terminate existing entities and produce new entities. The phenomenology concerns the behaviour of any single entity in conjunction with other entities, which is for the population balance modelling a reasonable description of the system (Ramkrishna & Mahoney, 2002). Regarding the hydrothermal crystallization process, a rigorous kinetic model for the solution precipitation and hydrothermal synthesis of $BaTiO_3$ particles based on mass and population balances has been recently proposed (Testino et. al., 2005). The population balances considered three elementary chemical kinetic processes: primary nucleation, secondary nucleation, and diffusion-controlled particle growth. Secondary nucleation accounts for the acceleration of the formation kinetics after an initial slow crystallization of $BaTiO_3$ particles. The time evolution of yield and particle size is represented by means of discretized mass and population balance equations. Hence, the algorithm is capable for calculating a generic number of conditions involved in the chemical reaction, which can optimize the crystallization and control the growth of $BaTiO_3$ particles. Another different approach based in a bi-variate population balance equations have prove to give more accurate results for the modelling of the barium titanate hydrothermal crystallization. The results obtained from the proposed population balance mathematical model clearly showed that such an approach can overcome the limitations of previous modelling work, and provide a useful tool for more detailed kinetic parameters estimation.

Moreover the model shows that secondary nucleation is indeed very important but particle aggregation cannot be neglected, these variables were not considered in the previous model (Marchizo, 2009).

Despite of the remarkable achievement to develop new strategies based on fundamental principles of thermodynamics and chemistry (reaction equilibrium and kinetics), caution should bear in mind for applying the proposed models to diverse hydrothermal systems and experimental situations. Hence, the estimation of kinetic parameters using population balance derived models could not be correct, these parameters can exhibit variations due to differences on temperature and concentration in the fluid media, which would lead to erroneous conclusions, because the reaction mechanism at certain conditions might change. Likewise, the population balance derived models assume that the system is well mixed and the crystallization rate is uniquely controlled by the chemical kinetics. These assumptions are generally valid for some small-scale laboratory reactors, but they fail in larger industrial plants where mixing is not well controlled. A mixing-limited precipitation rate is one of the problems commonly encountered in the scale-up of solid precipitation processes.

2.4.2 Hydrothermal crystallization process of selected oxide compounds

In the past, the term *hydrothermal crystallization* was used to referred it as nonconventional chemical process, this process involves heating an aqueous suspension of insoluble salts in an autoclave at temperatures and pressures greater than 100 ^{o}C and 0.1 MPa, respectively; resulting in the crystallization of the desired well-crystallized phases. This process, however, can be analogous to the term *hydrothermal synthesis* broadly used for physicists and chemists involved in this type of research, because both terms are related with the *genesis* of a specific compound. The crystallization process can mainly occur under very precise conditions of reaction, i.e. temperature, pressure, pH, concentration mineralizer or solvent solution. Thus, the hydrothermal crystallization method using inexpensive and chemicals easy to handle, can produce single or multicomponent oxides. The advantages of hydrothermal crystallization are the reduced energy costs due to the mild temperatures sufficient to achieve chemical reactions, less pollution, simplicity in the process equipment, and the fast rate of solid precipitation reactions (Vivekanandan & Kutty, 1989; Yoshimura & Suchanek, 1997; Riman et. al., 2002).

There are thousands of research works in the literature that include a vast experimental data related with the hydrothermal crystallization of metal oxides or inorganic compounds. The most popular among the metal oxides are those of perovskite oxides group, because of their wide application at the electronic industry. Hence, fundamental principles of crystallization of these materials are discussed in detail and compared with the present research experimental of the present authors regarding the crystallization of perovskite particles of $SrTiO_3$, $BaTiO_3$ and $La_{1-X}M_XCr_{1-Y}N_YO_3$.

2.4.3 Hydrothermal crystallization of perovskite derived oxides from gel precursors

In this section, we focus on the hydrothermal crystallization of perovskite-type structure oxide materials, because this particular group of oxides offers stupendous functional properties for a wide number of applications, in particular electronic applications. Perovskite compounds have the general formula ABO_3, and Perovskite is cubic structure in

nature which is shown in Figure 3, where the large A cations (Ba^{2+}, Sr^{2+}, Ca^{2+}, Pb^{2+}, La^{3+}, Bi^{3+} and K^{+}), but low in electric charge, are surrounded by 12 oxygens, whilst B ions relatively small in size (Ti^{4+}, Zr^{4+}, Sn^{4+}, W^{6+}, Nb^{5+}, Mn^{3+}, Mg^{2+}) are coordinated by 6 oxygens. The crystallization of the most representative compounds in this group, namely $BaTiO_3$ (BT), $SrTiO_3$ (ST) and solid solutions of $Ba_{1-X}Sr_XTiO_3$ (BST) or $PbZr_{1-X}Ti_XO_3$ (PZT) has been extensively studied under hydrothermal conditions.

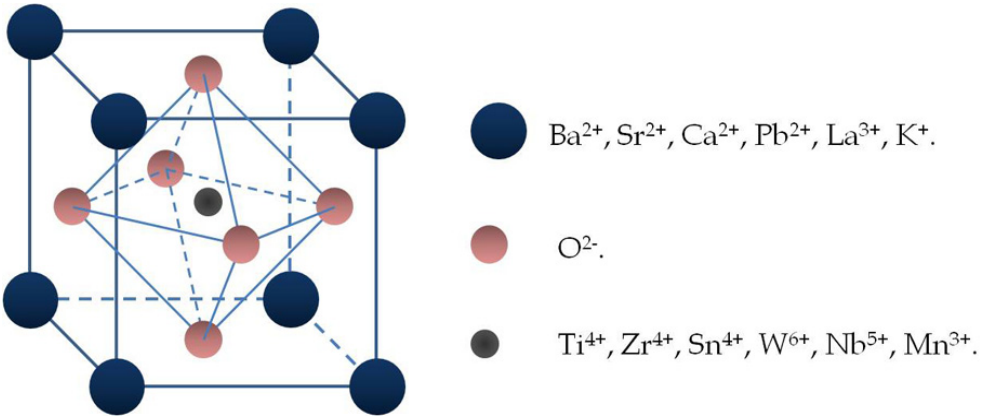

Fig. 3. Schematic representation of the unit lattice cell of the Perovskite cubic structure.

2.4.3.1 Hydrothermal crystallization of perovskite barium and strontium titanate oxides

$BaTiO_3$ (BT) and $SrTiO_3$ (ST) are the metal earth alkaline perovskite-like structures most prepared species under hydrothermal conditions, these compounds has similarity on the crystallization process as that proposed for PT. In terms of the chemical reaction equilibrium that can be produced on the hydrothermal system, and in accordance with the chemical reagent reactants that have been used the chemical reactions that are related with the crystallization of BT and ST powders are as follows:

Where M on chemical equations 3 and 4 is related to earth alkaline metals of the group IIA of the periodic table of elements, *viz.* Ca, Sr and Ba. The chemical reactions from 1 to 9 represent all the reaction equilibrium that are able to proceed in the system M-Ti-Na-H_2O and these reactions serve to produce the crystallization process, because they stem from the principal chemical reactions 1–12 that have widely investigated on the crystallization of BT under hydrothermal alkaline conditions and can operate on the case of the ST compound as well.

$$H_2O = H^+ + OH^- \quad (1)$$

$$H_2O(g) = H_2O \quad (2)$$

$$MTiO_3(s) + H_2O = M^{2+} + 2OH^- + TiO_2(s) \quad (3)$$

$$MOH^+ = M^{2+} + OH^- \quad (4)$$

$$Ti^{4+} + H_2O = TiOH_3^+ + H^+ \quad (5)$$

$$TiOH^{3+} + H_2O = Ti(OH)_2^{2+} + H^+ \quad (6)$$

$$Ti(OH)_2^{2+} + H_2O = Ti(OH)_3^{+} + H^+ \quad (7)$$

$$Ti(OH)_3^{+} + H_2O = Ti(OH)_4(aq) + H^+ \quad (8)$$

$$Ti(OH)_4(aq) = TiO_2(s) + 2H_2O \quad (9)$$

$$BaCl_2(aq) + TiCl_4(aq) + 6NaOH(aq) = BaTiO_3(s) + 6NaCl(aq) + 3H_2O(l) \quad (10)$$

$$Ba(OH)_2(aq) + TiO_2 \bullet xH_2O(s) + NaOH(aq) = BaTiO_3(s) + NaOH(aq) + xH_2O(l) \quad (11)$$

$$Ba(OH)_2(aq) + Ti(OH)_4 \bullet xH_2O(aq) + NaOH(aq) = BaTiO_3(s) + NaOH(aq) + 4xH_2O(l) \quad (12)$$

The chemical synthesis of BT particles has been studied over a broad range of experimental hydrothermal conditions; this compound is preferentially formed in highly concentrated alkaline solutions (pH > 10), as indicated by thermodynamic calculations in BT phase stability diagram proposed elsewhere (Lencka et. al., 1993; Riman et. al., 2002). The normal intervals of reaction time and temperature are 2–96 h and 120–250 ^{o}C where the crystallization is normally achieved, thus, the preparation of this type of powder is carried out in typical stainless steel 304 Teflon-lined autoclaves. Additional parametric variable studies recently conducted accounts for other variables that also have an effect on the formation of the BT pure phase like the molar ratio of precursor alkaline (KOH or NaOH) solvent (Vivekanandan & Kutty, 1989; Lee et. al, 2003) and the reactants ($Ba(OH)_2$ or titania source) (Moon et. al., 2003, Qi et. al., 2004), the Ba/Ti molar ratio of the raw materials (Wada et. al., 1995). Another specific studies recently conducted lead to remarkable analysis of the kinetic process related to the crystallization of BT particles and their growth (Walton et. al., 2001), and the control of the particle size and shape of the BT particles have been carried out by stirring the autoclave (Kubo et. al., 2009) and microwave assisted (Moreira et. al., 2008) hydrothermal methods.

Hitherto, in accordance with the analyses conducted based on experimental observations, indicate that the crystallization mechanism of BT particles is dissolution-precipitation in nature, and this mechanism is mainly controlled by the dissolving rate of the reactant solid specie, namely titania (oxide or amorphous gel). Thus, the presence of a high concentration of OH^- ions in the hydrothermal system is required to produce the hydrolysis of aqueous species, and these ions also seemed to act as catalysts to accelerate the transition from Ba-OH bonds, usually resulting on the crystallization of BT via precipitation that proceeds via the chemical reaction (13), resulting from the previous reaction (10–12) that is carried out during the earlier and intermediate stages of the hydrothermal treatment and are linked with the dissolution process.

$$BaOH^+(aq) + Ti(OH)_4^0(aq) = BaTiO_3(s) + 2H_2O + H^+(aq) \quad (13)$$

Once the solution is supersaturated due to dissolution of the precursor, precipitation of BT from the homogeneous solutions spontaneously occurs, yielding an abundant number of nuclei. Therefore, the dissolution of either titania hydrous amorphous or crystalline powders is the rate limiting step that controls the early stage of BT nucleation and growth

during the hydrothermal crystallization process, for anhydrous TiO_2 precursor, Ti-O bonds must be broken via hydrolytic attack to for hydroxyl-titanium complexes ($Ti(OH)_X^{4-X}$) capable of dissolution and reaction with barium ions or complexes (Ba^{2+} or $BaOH^+$) in solution to precipitate BT. Subsequently, the nuclei grow rapidly, resulting in an accelerated crystallization kinetics rate at the initial step of the process. In the solvent, the solute concentration decreases to below the supersaturation point as a result of this event, but remains sufficiently high for the particles to growth, avoiding a secondary nucleation. The particle coarsening proceeds during intermediate and final steps of the crystallization process, and mainly depends on the dissociation of the remaining reactants, or in some cases the separation of terminal organic groups that are liked to the Ti or Ba, e.g. acetiylacetone or acetate, these crystallization barriers serves to slow, if not halt, the kinetic rate in the final stage of the hydrothermal treatment (Eckert et. al., 1996). The crystallization studies indicates that the activation energy fro barium titanate crystallization under hydrothermal conditions varies on the range of 21-105 $kJmol^{-1}$, and the value of activation energy specifically depends on the type of compound used as titania source (Eckert et. al.; 1996; Walton et. al., 2001), but these values of activation are within the range of activation energy values for chemical reaction that proceed on the liquid stage.

On the other hand, major attempts recently conducted to investigate the crystallization of $SrTiO_3$ particles under hydrothermal conditions, have been designed by considering the fundamental principles derived from the synthesis of its related compounds, *viz.* BT or PT perovskite-like structure. A broad type of strontium titanate particle shapes, e.g. nanotube, dendrite, cuboidal and spherical; had been produced through optimizing the hydrothermal crystallization conditions by controlling parameter such as: the pH of the hydrothermal alkaline media in the range between 10–12 (Wendelbo et. al, 2006), reaction temperature and time. Furthermore, different chemical reagents including inorganic and organometallic had been employed as source of Sr^{2+} ($Sr(NO_3)_2$, $SrCl_2$, $Sr(OH)_2 \bullet 6H_2O$) and Ti^{4+} ($TiCl_4$, $TiO_2 \bullet H_2O$, $Ti(SO_4)_2$, $Ti(OC_4H_9)_4$, $Ti(OPr^i)_4$) for producing ST particles (Moon et. al., 1999; Zhang et. al., 2001; Wang et. al., 2009). Another factor that has been studied is related with the use of organic dispersants, namely polyvinyl alcohol, for controlling the crystallization of fine regular shaped ST particles. The dispersant that have large polymeric changes can operate as micelles that attract the hydrolysed ionic species that are formed during the hydrothermal treatment, this lead to and homogeneous nucleation and limited particle growth, resulting in the preparation of nanometer sized ST regular particles (Wei et. al., 2008). Regarding the mechanism correlated with the crystallization of ST particles, one model derived from further experimental data states that the dissolution-crystallization coupled with a second aggregative growth-recrystallization mechanisms are related with the bulk crystallization stage of ST particles under alkaline hydrothermal conditions, but is similar to that proposed for the formation of BT particles (Fig. 4). The second mechanism is achieved when heterogeneous nucleation promotes the formation of ST particles, the surface of the TiO_2 particles acts as the precipitation site for ST nuclei, and when the size of TiO_2 particles is reduced by the progressive dissolution, the aggregation growth of the ST particles proceeds in the reaction media. This phenomenon produces a marked particle agglomeration and also the coarsening of the particles can be promoted by the Ostwald recrystallization mechanism (Zhang et. al., 2004).

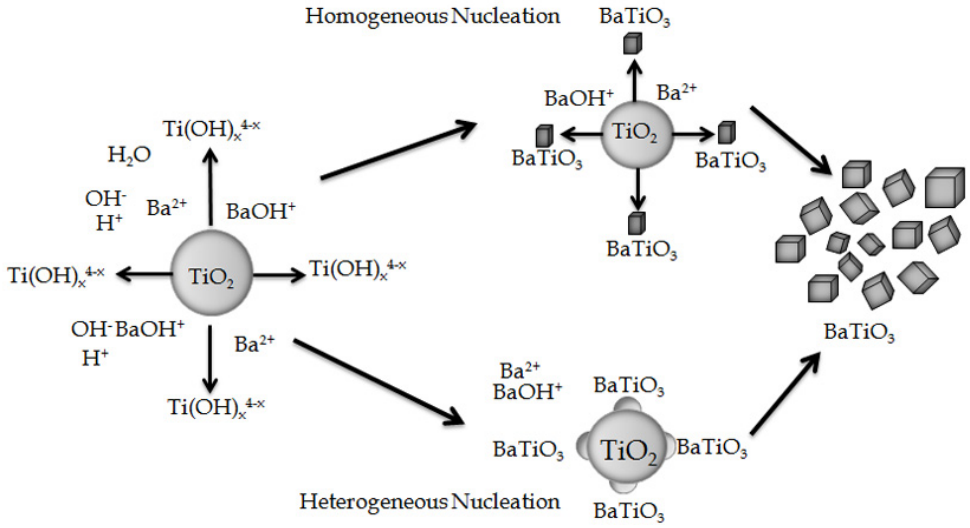

Fig. 4. Schematic sketch of the dissolution/precipitation mechanism that conduces to the hydrothermal crystallization of $BaTiO_3$ (Ecker et. al. 1996, Zhang et. al., 2004).

2.4.3.2 Single step hydrothermal crystallization of perovskite strontium and barium oxides using mineral precursors

In accordance to the former literature, in the last decade, the interest for using pure mineral species to produce pure synthetic inorganic compounds has been rising. In general, the synthesis of $SrTiO_3$ or $BaTiO_3$ has been broadly conducted by employing $Ti(OH)_4$ gel (Ti-gel), while several strontium soluble salts had been used as a source of Sr^{2+} ions. However, the challenge for employing low-grade chemical reagent precursors for preparing ABO_3 particles has not been considered yet. The approach for employing a pure mineral ore, like celestite ($SrSO_4$) or barite ($BaSO_4$) with a low grade of impurities; to produce strontium or barium compounds under hydrothermal conditions, was considered based on the analysis of the proposed chemical methods for producing functional ceramic materials and the former information related to the ionic substitution on mineral species, which are analogous to the mechanistic principles of hydrothermal crystallization discussed in this section. The employment of a low cost precursor may provide an additional advantage in order to propose an economical effective processing method.

Recently, the present authors have conducted an exhaustive efforts to develop a simple single step reaction method for the preparation of $SrTiO_3$, which involves the employment of a mineral $SrSO_4$ crystal plate (0.2 ± 0.0010 g, 6 ± 1 mm side and 2 ± 0.5 mm thick) with $Ti(OH)_4 \bullet 4.5H_2O$ gel (1 g, stoichiometric ratio Sr/Ti=1) under hydrothermal conditions, at various temperatures (150–250 °C) for different reaction intervals (0.08–96 h) in KOH solutions with different concentrations (5–10 M). The hydrothermal treatments were carried out in stainless steel micro-autoclaves lined with Teflon with a filling volume ratio of 50% of the total inner volume (30 ml). This process involves a complex solute dissolution stage because $SrSO_4$ is chemically stable even at acid, neutral and mild basic conditions. However,

the use of a mineral single crystal favours to analyse systematically the effect of the dissolution of this reactant coupled with the $Ti(OH)_4$ dehydration and serve to control the synthesis and crystallization kinetics of ST particles. Thus, the complete crystallization of ST particles in a single step of reaction occurred with the complete dissolution of the $SrSO_4$ crystal obtained at 250 ^oC for 96 h in a 5 M KOH solution, resulting in the formation of $SrTiO_3$ particles with two different shapes (peanut-like and cubic) as is shown in Figure 4. The parameter that has a marked effect on control the particle size and morphology is the temperature rather than the interval of reaction. ST particles having a bimodal size distribution (0.5–1 μm and 0.2–0.5 μm) were prepared at different temperatures for 96 h in a 5 M KOH solution from $SrSO_4$ crystals. The ST powders produced at mild temperatures (200 ^oC) were constituted by a large amount of agglomerated peanut-like shape irregular particles (Fig. 5a), together with a small amount of bulky crystals with a regular pseudo-cubic shape (1–4 μm). In contrast, at high temperature (250 ^oC), the pseudo-cubic (3–6 μm) ST particles exhibited a coarsening, while the amount of peanut-like shape (length = 1–5 μm and width = 0.5–1 μm) particles was significantly reduced (Fig. 5b). Hence, the coarsening of pseudo-cubic shaped particles is attributed to the Ostwald ripening particle growth mechanism (Peterson & Slamovich, 1999). Indeed, the growth of the aggregated particles is due to a recrystallization mechanism, which involves the dissolution of the primary small ST peanut-like particles produced at lower temperatures (< 200 ^oC). This process is promoted due to lower chemical stability that exhibits the strontium titanate oxide in highly concentrated (> 5 M) KOH solvent solutions at 250 ^oC. Another point that deserves to be emphasized is that related with the structural features of either peanut-like or cubic-like shaped particles. EDX spectra obtained on both particles did not show a marked difference on the molar Sr/Ti ratio, because the particles contain similar Sr and Ti amounts as it is suggested by the corresponding EDX spectrum in Fig. 5c (Rangel-Hernandez et. al., 2009).

In contrast, the increase on the surface area of the precursor $SrSO_4$ produces the control of morphology and size homogeneity for the ST particles. In general, the use of $SrSO_4$ powders with a narrow particle size distribution in the range from 25–38 μm, favoured the crystallization of very fine cubic ST particles, even at very short reaction intervals (0.08 h, Fig. 6a). However, ST powders with a bimodal size distribution, consisting of a large amount of pseudo cubic particles (0.75 μm) and a small quantity of large cubic particles (1.5 μm) were produced during intermediate reaction intervals between 3-12 h. In contrast, at the longest reaction interval of 24 h, the preferential formation of very fine pseudo-spherical ST particles (average size of 0.4 μm) was observed (Fig. 6b). The formation of the cubic particles is due to the crystallographic habit growth, which proceeded when the alkaline solvent reaches a supersaturation steady-state with the ionic species $Sr(OH)^+$ and $Ti(OH)_4^0$. Hence, a massive homogeneous nuclei formation and fast growth of the cubic particles proceeds in the hydrothermal system during intermediate reaction intervals. However, the ST cubic particles underwent into a preferential dissolution by increasing the reaction interval at long reaction period (24 h). The ST particle dissolution proceeds at high-energy faceted edges on the fine cubic particles, because of the relative low chemical stability of the ST perovskite structure in the concentrated alkaline media. This fact leads to further dissolution of the cubic particles and the recrystallization of the pseudo-spherical shaped particles from the solution.

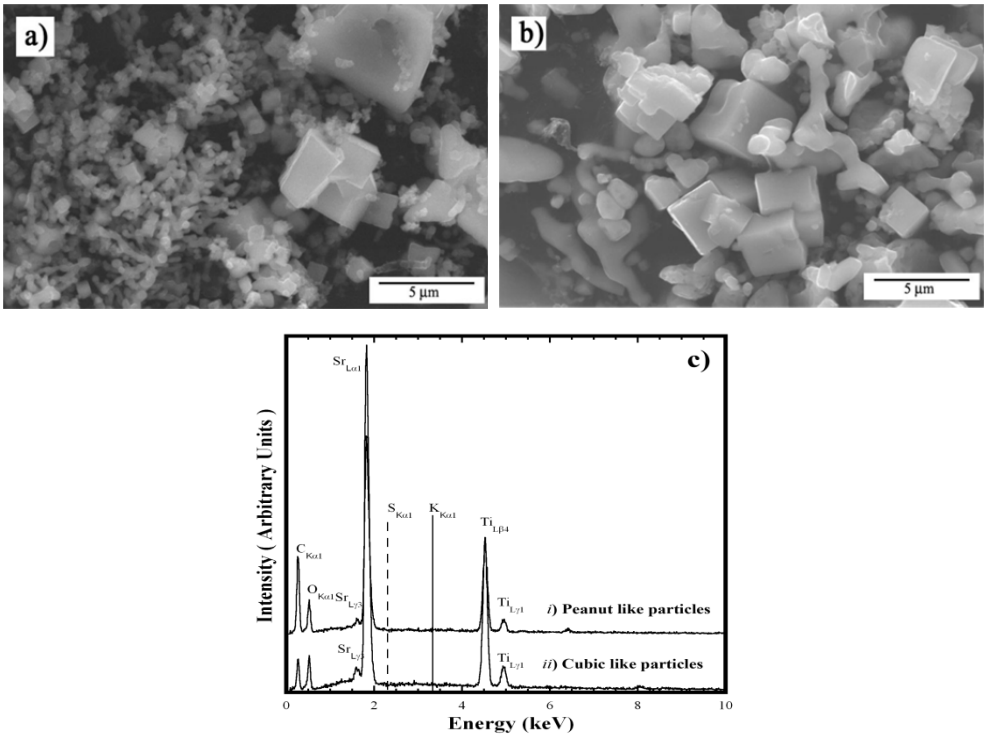

Fig. 5. Morphologies of ST particles obtained after hydrothermal treatments of $SrSO_4$ crystal plates, carried out at temperatures of (a) 200 °C, (b) 250 °C; and (c) EDX spectra of ST (*i*) peanut-like and (*ii*) cubic particles shown in Fig. 3b (Rangel-Hernandez et. al., 2009).

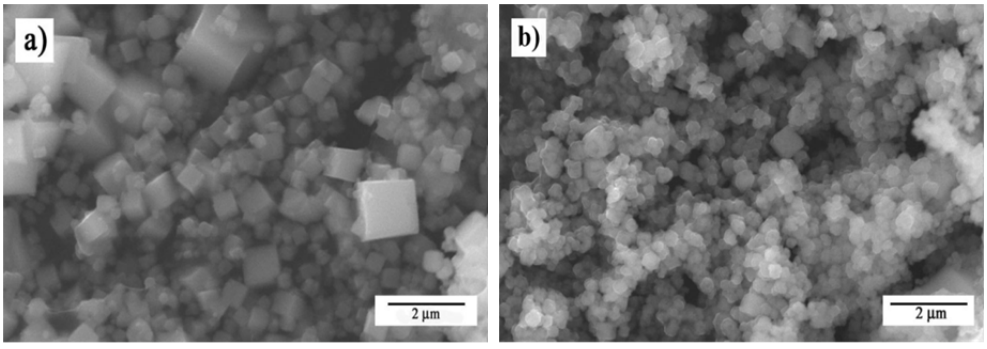

Fig. 6. $SrTiO_3$ particles hydrothermally produced using $SrSO_4$ powders at 250 °C in 5 M KOH solution for intervals of (a) 0.08 and (b) 24 h (Rangel-Hernandez et. al., 2009).

The bulk crystallization process of ST particles is dissolution-precipitation in nature, and the reaction path involving this mechanism that produces nuclei formation and crystal growth, is represented physically in the Figures 7a and 7b. These Figures gave the set of the original

$SrSO_4$ crystal plate embedded in the $Ti(OH)_4 \bullet 4.5H_2O$ gel prior the hydrothermal treatment and after 6 h of reaction at 200 °C. In terms of fundamental chemistry the reaction path way occurs trough the chemical equations 14 and 15:

$$SrSO_4(crystal) + Ti(OH)_4 \bullet 4.5H_2O(gel) + 2KOH = SrOH^+(aq) + K_2SO_4(aq) + Ti(OH)_4^0(aq) + 4.5H_2O + OH^-(aq) \quad (14)$$

$$SrOH^+(aq) + Ti(OH)_4^0(aq) + OH^-(aq) = SrTiO_3(s) + 3H_2O \quad (15)$$

Macroscopic aspects related with the single-step synthesis process were revealed during the early stages of the reaction at 200 °C for 6 h in a 5 M KOH solution (Fig. 7b). In general, the reaction gradually proceeds by the $SrSO_4$ crystal dissolution, the consumption of $SrSO_4$ occurs locally on those crystal surfaces exposed to the alkaline fluid and also on those crystal surfaces in contact with the Ti-gel. This phenomenon agrees with those results previously reported and provided evidences of the solubility of $SrSO_4$ compound in alkaline hydrothermal solutions (5 and 10 M NaOH) (Rendón-Angeles et. al., 2006). Hence, the continuous dissolution of the $SrSO_4$ crystal must yield the formation of $SrOH^+$ species (Eq. 14), because of the saturated alkaline conditions of the solvent. Indeed, the solubility of the Ti-gel is low in high concentrated KOH (> 0.1 M) solutions (Wang et. al., 2009, Rangel-Hernandez et. al., 2009). However, the consumption of the $SrSO_4$ crystal dissolution (α) was markedly reduced due to the presence of the Ti-gel (Fig. 7c). This fact let us to conclude that the reactivity of Ti-gel is the limiting rate variable for crystallization, because reduces the dissolution rate of the $SrSO_4$ phase. Thus, the equation (4) is proposed for the crystallization of ST and is similar to that discussed at the early part of the present section for PT and BT compounds. The nucleation and growth processes of the ST particles occur when the alkaline (KOH) solution reaches a supersaturation steady-state of the species $Sr(OH)^+$ and $Ti(OH)_4^0$. The ST particles precipitation locally occurred at Ti-gel surface and between the spaces with the remaining $SrSO_4$ crystal, because the mass transport was limited during the treatments, which were conducted under neither agitation nor thermal gradients. Additionally, kinetic data obtained from $SrSO_4$ consumption curves depicted that the activation energy required for the synthesis of $SrTiO_3$ powders from the complete consumption of an $SrSO_4$ crystal plate under hydrothermal conditions, is 27.9 kJ mol^{-1}. One particular fact that must be emphasised is related with the incorporation of the major impurities on the ST particles during the synthesis process, namely Ba (5.7 wt.%) and CO_3^{-2} (0.6 wt.%), contained in the $SrSO_4$ crystals, does not proceed during the crystallization event because neither the presence of barium nor carbonate compounds were found on the compositional analysis conducted by EDX and DRX techniques in the ST particles.

On the other hand, the crystallization of perovskite related compounds like ST or BT via the transformation of sulphate alkaline earth metal mineral species is hinder for the barite mineral. The crystalline transformation of $BaSO_4$ to $BaTiO_3$ was studied using the single step reaction route aforementioned; and the high chemical stability (low solubility) of the orthorhombic structure limited the dissolution of the barite crystals under hydrothermal conditions even in highly concentrated KOH solutions (>5 M). The reactivity of the orthorhombic structure with the alkaline solvent can be influenced by the size of the alkaline earth metal ion incorporated in the structure, these results are in agreement with those early reported on the transformation of Ca, Sr and Ba-chlorapatite crystals into their respective hydroxyapatite species (Rendón-Angeles et. al., 2000a). This factor reduces the rate of the BT

particle crystallization process, but the reaction was conducted by increasing the concentration of the KOH solution up to 10 M, and the complete dissolution of the $BaSO_4$ crystal occurred for large reaction intervals of 144 h above 200 °C. Optimum steady-state supersaturation of the solvent media with Ba^{2+} and Ti^{4+} ions that achieve the conditions for homogeneous nucleation of BT particles were found to proceed at temperatures below 200 °C (Figure 8). Fine BT particles with pseudo-cubic, star-like and dendrite shapes were preferentially formed in 10 KOH. At sever treatment conditions of temperature 250 °C for 144 h, the $BaSO_4$ crystals were completely dissolved, and the formation of reaction by-products Ba_2TiO_4 (needle crystals in Figure 8c) and a few amount of TiO_2 simultaneously occurred with the excessive growth of polyhedral aggregated BT crystals. This particular behaviour is attributed to the differences in the chemical reactivity of the alkaline solution resulting in different dissolving rates for solid species, this can shift the reaction equilibrium coupled with the saturation conditions. Therefore, other crystalline phases are able to precipitate because thermodynamically are more stable than BT.

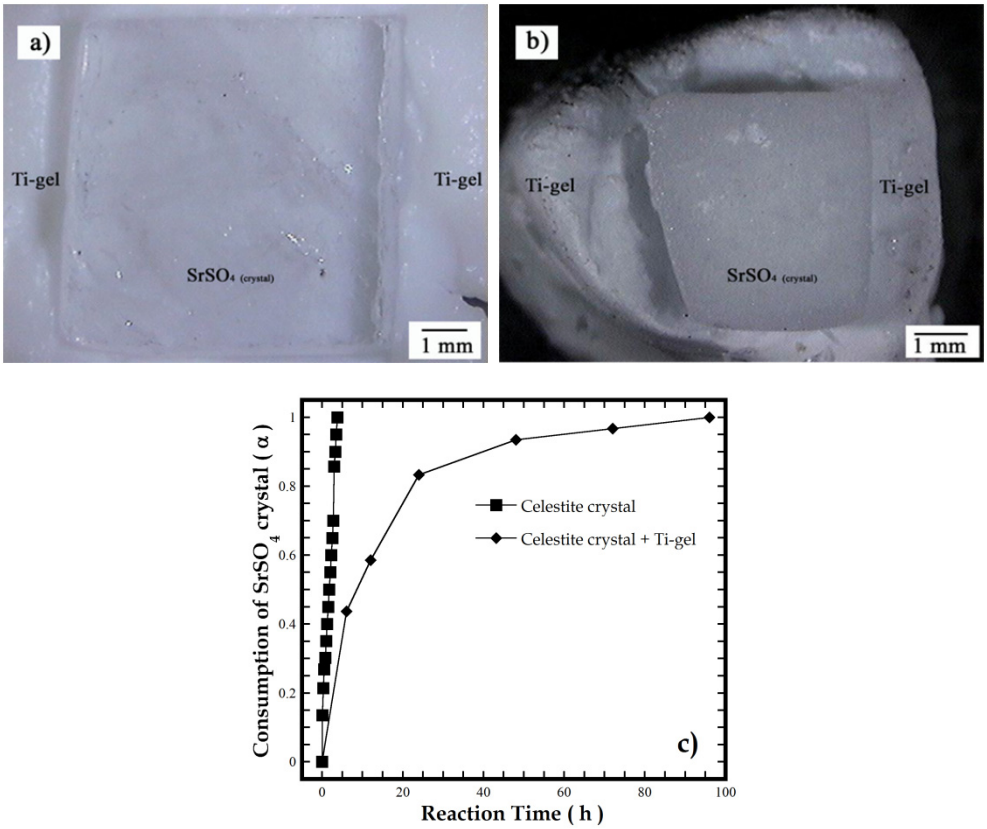

Fig. 7. Aspects of (a) original $SrSO_4$ crystal plate embedded in Ti-gel, and (b) the partially reacted $SrSO_4$ crystal and Ti-gel at 200 °C for 6 h in a 5 M KOH solution. (c) Consumption curves (α) of $SrSO_4$ crystal vs. the reaction interval obtained at 250 °C in a 5 M KOH solution, (■) without Ti-gel and (◆) with Ti-gel additions (Rangel-Hernandez et. al., 2009).

2.4.3.3 Elimination of mineral impurities during the synthesis of strontium titanate particles under hydrothermal conditions

Regarding the presence of high content of impurities during the crystallization of ST particles from mineral celestite ores. The experimental research work conducted recently by the authors of the present chapter; clearly contribute to demonstrate that refining of the major metal ion contained in the mineral ore proceeds during the hydrothermal crystallization of ST powders. Thus, the chemical stability of the barite-celestite mineral specie was investigated to elucidate the feasibility to conduct simultaneously the crystallization of ST particles and the release of major impurities such as Ba, and the preparation of BT powders as well. In particular, the barite-celestite mineral consists in a solid solution with a general chemical formula of $Sr_{0.70}Ba_{0.30}SO_4$, which was determined by wet chemistry using ICP, the total content of major constituents $SrSO_4$ and $BaSO_4$ was 64.7 wt.% and 35.3 wt.%, respectively. Additional microprobe wavelength X-ray diffraction analyses conducted by scanning electron microscope observations indicated that the microstructure of the mineral consists of two major solid solutions, one rich in strontium $Sr_{0.95}Ba_{0.05}SO_4$ and a less amount of an intermediate $Sr_{0.75}Ba_{0.25}SO_4$. The hydrothermal treatments of barite-celestite crystal plate samples were conducted in accordance with the experimental procedure explained before for high pure celestite crystals.

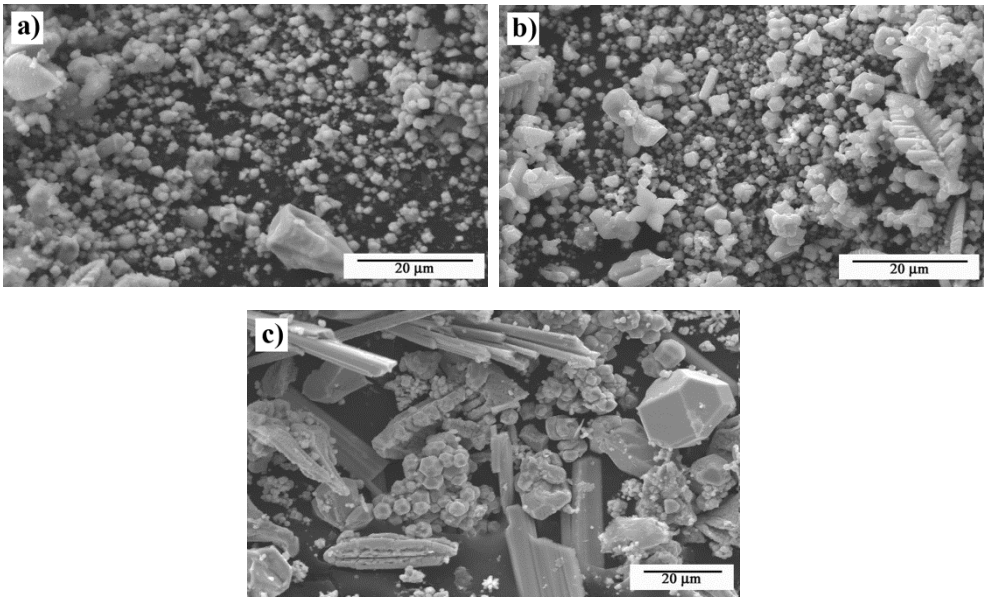

Fig. 8. $BaTiO_3$ particles crystallized from barite mineral plates in a 10 M KOH solution for 24 h at temperatures of (a) 150, (b) 200 and (c) 250 ^oC.

The synthesis of ST particles was preferentially obtained using the barite-celestite crystals in a feedstock alkaline 5 M KOH solution; the transformation of the mineral specie into the perovskite oxide is strongly affected by the temperature and concentration of the solvent media rather than the reaction interval. Marked morphological and particle size differences

were derived due to the increase of reaction temperature, a mixture of fine particles resembling cubic and start-like shapes were formed at mild temperatures (150 and 200 ^{o}C) for 12 h, increasing the temperature at 250 ^{o}C bulky aggregated cubic ST particles (20 μm size) were crystallized (Figure 9). During the hydrothermal crystallization of the ST compound the incorporation of the Ba^{2+} ions was avoided to occur in the structure of ST particles, this is supported by the EDX spectra of the cubic and star-like ST particles where no traces of Ba are visible (Fig. 9d).

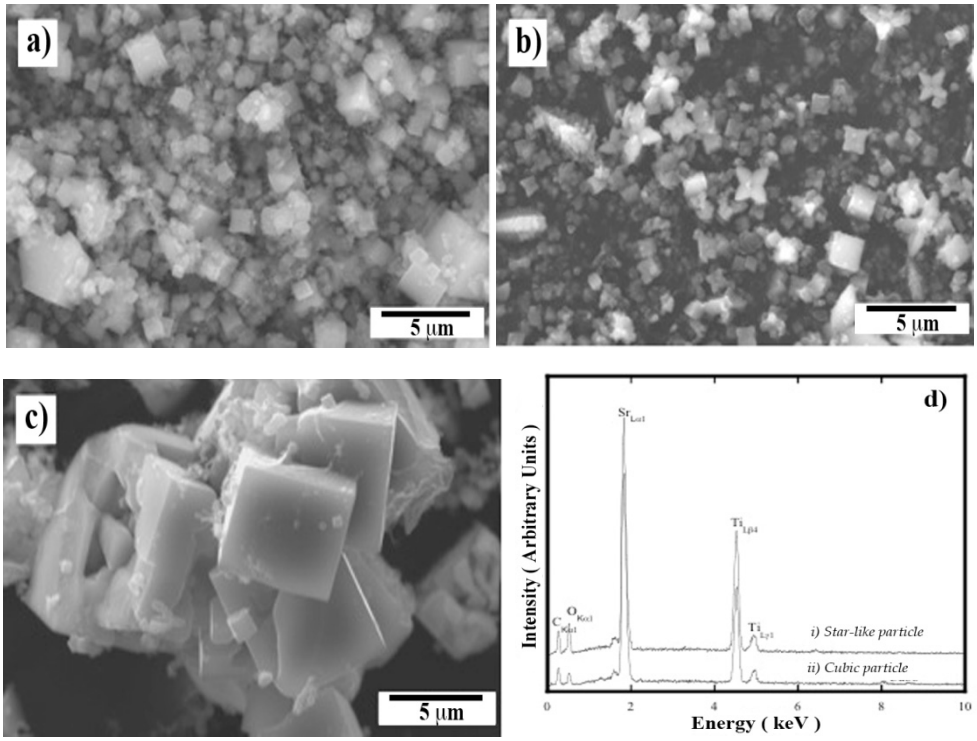

Fig. 9. $SrTiO_3$ particles crystallized from barite-celestite mineral plates in a 5 M KOH solution for 12 h at different temperatures of (a) 150, (b) 200 and (c) 250 ^{o}C. (d) EDX spectra of the ST particles shown in (b).

Two main factors are associated with; one is related to the marked compositional gradient differences of the metal ions Sr^{2+} and Ba^{2+} produced in the solvent media during mineral dissolution, coupled with the stability of Ba^{2+} to form complexes ions in alkaline solutions ($BaOH^{+}$, Eq. 4). Indeed, wet chemical analyses of the remaining solutions after the treatments gave evidences that support the above inference, because the Ba^{2+} ions content gradually increased as far as the complete mineral dissolution was concluded for 96 h at 250 ^{o}C. The content of Ba determined by in the solution was 20.0 ± 0.8 wt%, which is nearly the same, measured in the original barite-celestite crystals (20.8 wt%). The ST particles crystallization proceeds by the same model established previously on the case of the transformation of high pure celestite crystal to ST particles, the control of morphology and

particle size for the ST powders can be optimized by limiting the dissolution-recrystallization mechanism that operates at sever treatment conditions of temperature (T> 200 ^{o}C) and long periods (t> 72 h). Therefore, these results probe that the hydrothermal technique combined with the use of mineral (pure and contaminated) as precursor for the synthesis of inorganic materials can be an attractive technique to be explored at an industrial scale.

2.4.3.4 Hydrothermal crystallization of perovskite lanthanum chromite oxides

Lanthanum chromite ($LaCrO_3$, LC) powders substituted with alkaline metals (Ca or Sr) have been widely accepted as the candidate for interconnection materials in Solid Oxide Fuel Cells (SOFCs) and also particular solid solutions can be used as oxygen sensor at high temperature (Chakraborty et. al., 2000) The partial substitution of lanthanum ions with alkaline metal ions, Ca or Sr in the A site of La, increases the chemical stability and electric conductivity, whilst Al or Ni in the B site reduces the thermal expansion coefficient at high temperature, when compared with the properties of pure lanthanum chromite (Ianculescu, et. al., 2001). Hitherto, various chemical routes have been used to process lanthanum chromite powders (Bliger. et. al., 1997). However, these chemical processes involve heat treatments at temperatures beyond 700 °C, in order to obtain the crystalline phase pure phase and their solid solutions with Ca or Sr in the A site and Ni or Al in the B in the sites of the perovskite-like structure ABO_3. Hence, the present authors recently determined through exhaustive research work, the aspects related to the crystallization of precursor complex gel of the $La_{1-X}M_XCr_{1-Y}N_YOH_{6-x}$ compound into their respective perovskite solid solutions $La_{1-X}M_XCr_{1-Y}N_YO_3$ (where M = Ca or Sr and N = Al or Ni) with orthorhombic crystalline structure under hydrothermal conditions, at a temperature range between 350–500 °C for short reaction intervals (0.5–2 h).

The precursor complex gel was prepared by the alkaline coprecipitation method widely used to prepare this type of materials; the details of the chemical preparative method are given elsewhere (Inagaki et. al., 1990). Precursor lanthanum chromite complex gels were prepared by employing reagent grade chemicals of: $LaCl_3 \bullet 7H_2O$ (99.998%), $Cr(NO_3)_3 \bullet 9H_2O$ (99.9%), $CaCl_2 \bullet 2H_2O$ (99%), $SrCl_2 \bullet 2H_2O$ (99%), $Ni(NO_3)_2 \bullet 6H_2O$, $Al(NO_3)_3 \bullet 9H_2O$ and NaOH (99.998%) (Wako Pure Chemical Industries, Ltd., Japan). Aqueous solutions with a concentration 0.05 M of $LaCl_3$, $Cr(NO_3)_3$ and $CaCl_2$ were prepared with deionized water, and a solution of 0.5 M of NaOH was employed as coprecipitation media. In a typical procedure, a volume of 475 ml of the precipitating solution (NaOH) was poured in a biker, and chromium or the mixtures of Cr+Al, Cr+Ni; solution (500 ml) was then mixed, which results in the formation of an opaque whitish green precipitate ($Cr(OH)_3$, or $Al(OH)_3$, $Ni(OH)_2$), which was subsequently dissolved by vigorous stirring. Finally, the coprecipitation of the complex gel was carried out by the addition of the same volume (500 ml) of the solution containing the other elements, La or the mixture of La+Ca, La+Sr. The solutions were mixed in different volumetric ratios, La:M:Cr:N, 1:0:1:0, 0.9:0.1:1:0 and 0.8:0.2:1:0, 1:0:0.95:0.05; 1:0:0.9:0.1; 0.8:0.2:0.95:0.05, 0.8:0.2:0.9:0.1; which matches the compositional stoichiometric of the solid solutions, $LaCrO_3$, $La_{0.9}Ca_{0.1}CrO_3$, $La_{0.8}Ca_{0.2}CrO_3$, $La_{0.8}Sr_{0.1}CrO_3$, $La_{0.8}Sr_{0.2}CrO_3$, $LaCr_{0.95}Al_{0.05}O_3$, $LaCr_{0.9}Al_{0.1}O_3$, $LaCa_{0.2}Cr_{0.95}Al_{0.05}O_3$, $LaCa_{0.2}Cr_{0.9}Al_{0.1}O_3$, $LaSr_{0.2}Cr_{0.95}Al_{0.05}O_3$, $LaSr_{0.2}Cr_{0.9}Al_{0.1}O_3$, $LaSr_{0.2}Cr_{0.95}Ni_{0.05}O_3$, $LaSr_{0.2}Cr_{0.9}Ni_{0.1}O_3$. The coprecipitated gel was centrifuged and a volume of 20 ml was then poured into a hydrothermal Hastelloy C-lined microautoclave (40 ml capacity, Figure 10). The vessel was heated at a constant rate of 20 ^{o}C/min up at various temperatures (350–500

°C) for a reaction interval between 0.5 and 2 h. After the treatments, the precipitates were well washed with distilled water, decanted and then dried in an oven at 100 °C overnight (Rivas-Vázquez et. al., 2004, 2006; Rendón-Angeles et. al., 2009).

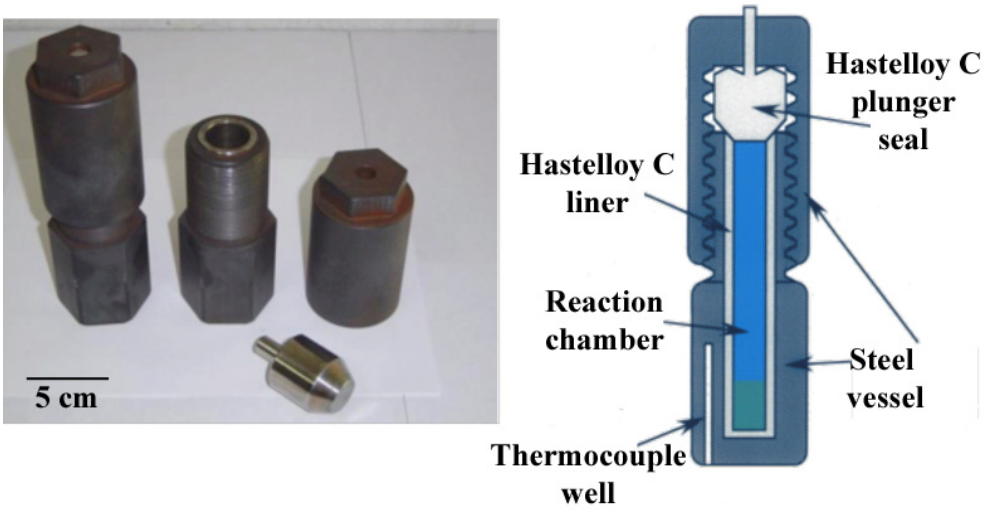

Fig. 10. Typical Hastelloy C type lined microautoclave and scheme of the cross section of the vessel, which was employed for conducting the synthesis of perovskite lanthanum chromite powders under hydrothermal conditions.

The minimum temperature for conducting the crystallization of the pure LC powders was 375 °C for a reaction interval of 1 h. This parameter, however, is mainly affected by the incorporation of the metal ions in both A and B sites of the perovskite structure ABO_3, and also with the amount of metal dopant ion inserted. Thus, the crystallization of powders corresponding to the solid solutions $La_{1-X}M_XCr_{1-Y}N_YO_3$ (where M = Ca or Sr and N = Al or Ni) was observed to proceeds at temperatures above 400 °C, when only a 10 mol% of Ca^{2+} or Sr^{2+} were partially substituting La^{3+} site. Thus, in the particular case of the $La_{0.9}Ca_{0.1}CrO_3$ and $La_{0.8}Ca_{0.2}CrO_3$ solid solutions, the structural analyses in Figure 11a depicted that at a constant reaction interval 1 h, the powders of $La_{0.9}Ca_{0.1}CrO_3$ were produced at a temperature of 400 °C without contaminant formation, in contrast with the $La_{0.8}Ca_{0.2}CrO_3$ powders that were produced together with a marked amount of secondary crystalline phases of $La(OH)_3$, CrOOH, and $CaCrO_4$, these phases were eliminated by increasing the reaction temperature up to 425 °C resulting in the crystallization of the pure phase $La_{0.8}Ca_{0.2}CrO_3$. This behaviour was also determined for the crystallization of the $La_{0.9}Ca_{0.1}CrO_3$ and $La_{0.8}Ca_{0.2}CrO_3$ powders. The minimum temperature that achieves the perovskite powders formation was found to increase at 450 °C, when Al^{3+} partially substituted Cr^{3+} sites. This situation is more critical when two different metal dopants were simultaneously incorporated at the same time to form a complex oxide such as; $LaCa_{0.2}Cr_{0.95}Al_{0.05}O_3$ and $LaCa_{0.2}Cr_{0.9}Al_{0.1}O_3$, the powders corresponding to these LC solid solutions were obtained at minimum temperature of 475 °C, which is a significant increase (100 °C) when compared with the low temperature needed to form the pure $LaCrO_3$. The significant variation on the processing parameters

experimentally determined, namely the temperature, can be associated with the thermodynamic fundamental principles, e.g. the Gibbs free energy. The calculus of the ΔG values for the formation of Ca and Sr doped LC solid solutions over a wide range of temperature (Fig. 11b), are in a good agreement with the trend of the experimental results aforementioned. Because, in terms of energy, the crystallization reaction that required less energy consumption is that leads to the formation of pure $LaCrO_3$, compound that exhibit the lowest ΔG values in comparison with those of $La_{0.9}M_{0.1}CrO_3$ and $La_{0.8}M_{0.2}CrO_3$ solid solutions (M= Ca^{2+} or Sr^{2+}).

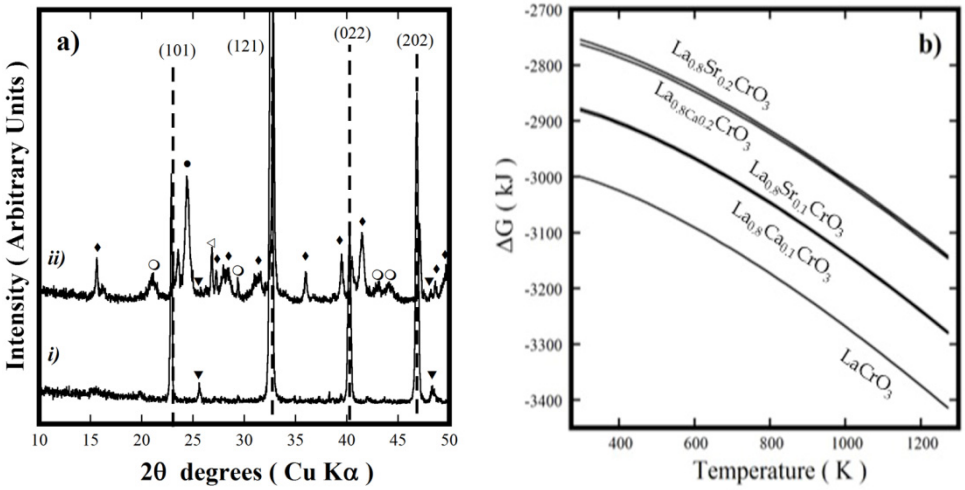

Fig. 11. (a) X-ray diffraction patterns of (*i*) $La_{0.9}Ca_{0.1}CrO_3$ and (*ii*) $La_{0.8}Ca_{0.2}CrO_3$ powders produced at 400 °C for 1 h. $LaCrO_3$ (JCPDS 33-701) compound doted line; (◆) $La(OH)_3$, (◁) CrOOH, (●) $CaCrO_4$, (▼) low intensity peaks of $LaCrO_3$. (b) Variation of the ΔG formation for pure $LaCrO_3$ and $La_{0.9}M_{0.1}CrO_3$ and $La_{0.8}M_{0.2}CrO_3$ solid solutions (M= Ca^{2+} or Sr^{2+}).

Morphological aspects of powders corresponding to the solid solutions of $La_{0.9}M_{0.1}CrO_3$ and $La_{0.8}M_{0.2}CrO_3$ (M= Ca^{2+} or Sr^{2+}) solid solutions obtained at 400 and 425 °C, respectively; are shown in Figure 12. Particles with submicron size and irregular morphology, which resembles a peanut-like shape, were preferentially formed on all cases investigated, it is also indicated that the particle morphology of these compounds is irrespective of the gel crystallization temperature. Furthermore, the particles showed a marked agglomeration due to its particular morphology and particle size aspect. One point that deserves emphasis is that related with the marked tendency for particle bounding that underwent the particles. These are reliable evidences that indicate the particles of the formed LC solid solutions were partially dissolved in the fluid at an intermediate reaction stage (>1 h) of the hydrothermal treatment, once the secondary crystalline phases were completely exhausted.

This phenomenon seems to occur markedly on the $La_{0.8}Sr_{0.2}CrO_3$ particles (Fig. 12d) hydrothermally synthesized 1 h at 425 °C, because these particles exhibit the smallest particle size (average 250 nm) in comparison with the other three powders that have an average particle size of 350 nm (Figs. 12a-12c). This fact can be explained based on the

chemical stability of the crystalline phase, which must be low and therefore the dissolution proceeds rapidly. Indeed, this inference is supported by the fact that the amount of regular $La_{0.8}Sr_{0.2}CrO_3$ particles is further decreased in this particular powder. Although, the particles exhibited a non-peculiar morphology when compared with those used for preparing dense advanced ceramic materials, it was experimentally probed that these fine powders have better sinterability features even in oxidizing atmospheres (Rivas-Vázquez et. al., 2004, 2006; Rendón-Angeles et. al., 2009).

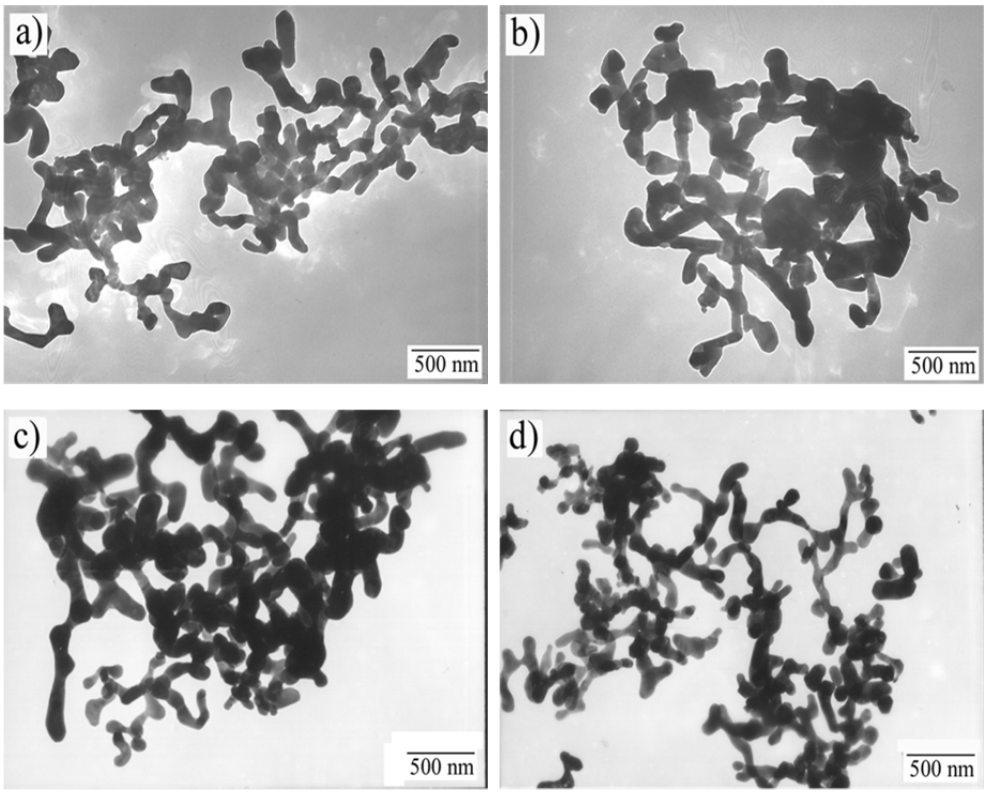

Fig. 12. Transmission electron micrographs of hydrothermally produced powders for 1 h at 400 °C (a) $La_{0.9}Ca_{0.1}CrO_3$ and (c) $La_{0.9}Sr_{0.1}CrO_3$; and 425 °C (b) $La_{0.8}M_{0.2}CrO_3$ and (d) $La_{0.8}M_{0.2}CrO_3$.

The details of the reaction pathway that are linked to the crystallization of the final tailored LC composition were determined during the preparation of $La_{0.9}Ca_{0.1}CrO_3$ solid solution. Preliminary observations conducted even during the heating stage of treatment confirmed that the hydrothermal crystallization involves a preliminary reaction stage, which is related with the dehydration process of the complex gel and proceeds at temperatures above 300 °C, resulting on the autogeneous formation of hydrothermal solvent inside the reaction vessel. The pH of the remaining solutions after the hydrothermal treatment varied in the range between 7.2-7.8, which confirms that the crystallization of the lanthanum chromite powders

was conducted in low alkaline conditions. Once the treatment temperature is reached (400 ^{o}C), as a result of the complex gel dehydration process, the crystallization of intermediate secondary phases proceeded during the earlier stages of the reaction (10–30 min). The major stable secondary phases that were produced during this reaction interval range were $La(OH)_3$, CrOOH, which correspond to the needle and platelets, respectively (Figs. 13a–13b); these observations are in a good consistence with the X-ray diffraction patterns of the powders produced at 400 ^{o}C for different reaction intervals (Fig. 13d), these results also showed the presence of a slight amount of $CaCrO_4$. The dissolution of the reaction by-products is fast in such a diluted alkaline hydrothermal media. Hence, the nucleation of the oxide particles proceeds preferentially at the surface of the remaining complex gel during the dehydration process, because the crystallization by the process employed in this study proceeded at higher temperatures (300–450 ^{o}C) than those determined for $LaCrO_3$ and $La_{0.5}Sr_{0.5}MnO_3$ particles under concentrated alkaline hydrothermal conditions (8 M KOH), 240 and 260 ^{o}C, respectively (Zheng et. al., 1999; Spooren et. al., 2003). The complete crystallization of $La_{0.9}Ca_{0.1}CrO_3$ particles was even promoted for a shorter interval as 1 h, resulting in the formation of irregular particles resembling peanut-like shapes (Fig. 13c).

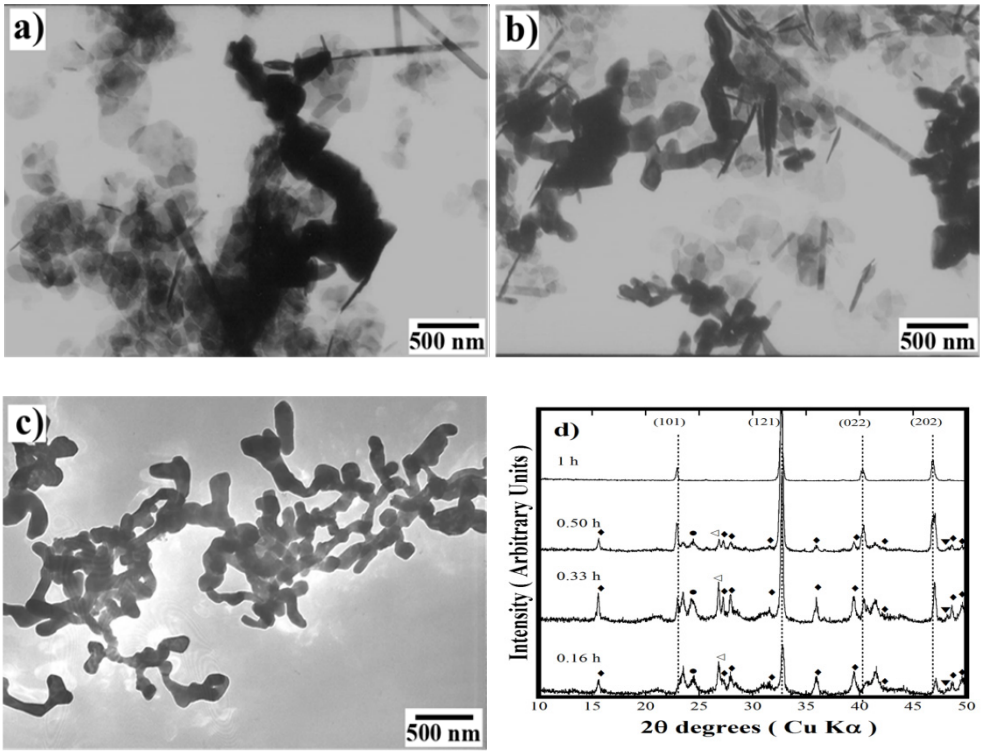

Fig. 13. TEM micrographs of the reaction products obtained under hydrothermal conditions at 400 ^{o}C for different intervals (a) 0.33, (b) 0.5 and (c) 1 h. (d) X-ray diffraction patterns of complex gel corresponding to the above micrographs. $LaCrO_3$ (JCPDS 33-701) compound doted line; (◆) $La(OH)_3$, (◁) CrOOH, (●) $CaCrO_4$, (▼) low intensity peaks of $LaCrO_3$.

Regarding the peculiar morphology of the $La_{0.9}M_{0.1}CrO_3$ and $La_{0.8}M_{0.2}CrO_3$ solid solutions (M= Ca^{2+} or Sr^{2+}). Two main factors promoted the formation of the peanut-like shaped particles (Figure 14); the first is related with the nucleation and growth process which proceeded very fast for reaction intervals of 0.5 up to 2 h at interval of temperatures (400–450 ◦C) and limited the growth of $La_{1-X}M_XCrO_3$ particles. The second one is associated with the concentration of the solvent media; the alkaline fluid autogenously formed during the hydrothermal treatment is not capable of achieving the actuated conditions that lead the crystallization of particles with cubic habit (Zheng et. al., 1999; Spooren et. al., 2003). However, the $La_{1-X}Sr_XCrO_3$ particles were partially dissolved in the solvent media at high temperature (400–450 °C), resulting in a marked particle joining by developing necks on the surfaces of primary synthesized particles in contact, as shown in Figure 14 for $La_{0.8}Sr_{0.2}CrO_3$ powders.

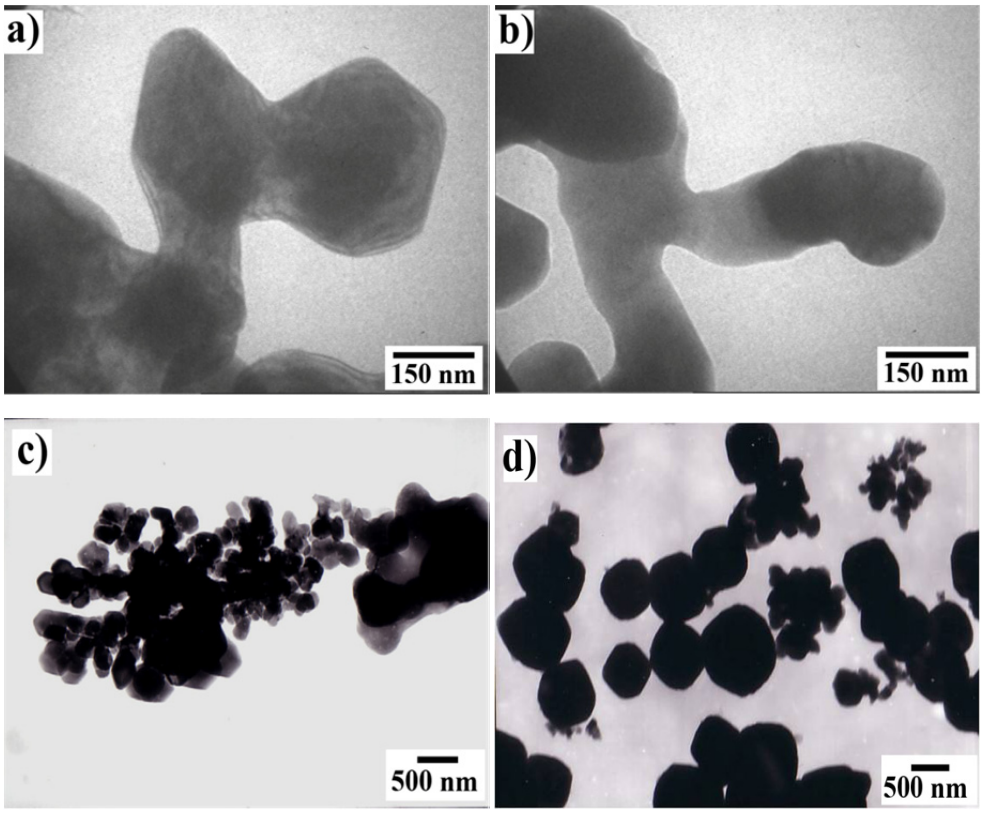

Fig. 14. Transmission electron micrographs of $La_{0.8}Sr_{0.2}CrO_3$ powders obtained at 450 °C for reaction intervals of (a) 1 and (b) 2 h. $La_{0.8}Sr_{0.2}Cr_{0.9}Al_{0.9}O_3$ powders prepared at 475 °C for 1 h in NaOH solutions of (c) 0.1 and (d) 5 M using as a precursor dried complex gel.

The local recrystallization of the solute is mainly promoted inside the reaction vessel, due to the fact that no fluid convection occurred during the hydrothermal treatment, because the treatments were conducted under static conditions at constant temperature, therefore, mass

transfer due to convection was further limited (Bayrappa & Yoshimura, 2001). Hence, the crystallization mechanism is similar to that described previously for other perovskite species, but it differs on the rate of kinetics that lead to produce particles particular aspect. In contrast, the particle bonding was limited by modifying the treatment conditions, using a dried complex gel $La_{0.8}Sr_{0.2}Cr_{0.9}Al_{0.1}O_3$ and different aqueous solvent media (water, KOH, NaOH and KF), resulting in the optimum control of dissolution and crystallization of fine particles with regular. A marked particle growth, however, was determined as a result of increasing the concentration of the alkaline solution from 0.1 to 5 M (NaOH or KOH). The formation of submicron particles monodispersed (0.5 – 0.75 μm) was found to proceed on these solvents (Figs. 14c, 14d). Furthermore, the employment of the alkaline solvents NaOH and KF leads to the crystallization of pseudo-cubic shaped and hexagonal plate particles, respectively; the differences on the particle morphology control are due to the chemical reactivity of the different solutions with the dried complex gel.

2.5 Replacement reactions on minerals species under hydrothermal conditions as a new approach for preparing inorganic materials

Another different approach similar to the mineral transformation into perovskite oxide powders was investigated to establish an alternative processing route for mineral ores via controlled dissolution-precipitation. The precursor mineral considered were the alkaline earth sulphates of $SrSO_4$ and $BaSO_4$, for preparing high pure strontium inorganic compounds, namely $SrCO_3$, $BaCO_3$, $SrCrO_4$, SrF_2, $Sr(OH)_2$. This chemical preparative method involves the dissolution–recrystallization mechanism, similar to the process that achieves the ionic replacement reaction in mineral ores, and promotes the conversion of natural ores at the earth's crust into more chemically stable mineral species or inorganic compounds (Putnis, 2002, 2009). The development of more efficient and environmental friendly chemical routes has recently been under concern of some researchers. The new chemical techniques or the optimized conventional routes might lead to reduce the pollution grade of contaminants, which is produced during mineral processing stages. The related alkaline earth sulphate minerals, such as $SrSO_4$ and $BaSO_4$, have been exploited since several decades, because these are the main source of the alkaline earth metals elements, Sr and Ba, and are used as a main source for preparing inorganic compounds of Sr and Ba. During the last decade, some attention has been paid to the use of celestite ore for producing functional ceramic compounds with magnetic properties, e.g. strontium hexaferrite ($SrFe_{12}O_{19}$); two different methods were proposed, coprecipitation in aqueous solutions via mineral powder leaching and powder mechanochemical activation techniques (Hessien et. al., 2009; Tiwary, et. al. 2008). Hence, since a decade, the present authors have devoted efforts in order to investigate, from a different approach of preparative chemistry; the nature of the possible replacement reactions that can be achieved under hydrothermal conditions, as was found to proceed even in synthetic inorganic compounds (Rendón-Angeles et. al., 2000b). This could derive in an optimum method for preparing high grade Sr and Ba compounds. The most relevant aspects found regarding this topic are given in this section.

2.5.1 Aspects of the compositional and structural transformation on sulphate minerals under alkaline hydrothermal conditions

Hitherto, the ion exchange reaction of SO_4^{2-} ions with CO_3^{2-} ions has been one of the subjects of research work, which involves both mineral celestite ($SrSO_4$) and barite ($BaSO_4$) species.

This particular transformation involves the conversion of MSO_4 into MCO_3, M= Sr or Ba, because these carbonated compound are widely used as a precursors for the preparation of strontium and barium inorganic compounds (Suaréz-Orduña et. al., 2004a; Rendón-Angeles et. al., 2008). Preliminary evidences of the ion exchange replacement process were investigated on the mineral celestite specie, thermodynamic and kinetic details were reported elsewhere (Yoshino et. al., 1985). The exchange of SO_4^{2-} ions with CO_3^{2-} ions was investigated on large mineral $SrSO_4$ bulky crystal plates, which were leached at low temperature (55 ^oC). The ion replacement was achieved by two reaction mechanisms, at initial and intermediate stages, the superficial reaction and the diffusion of SO_4^{2-} ions produced a dense $SrCO_3$, the complete ion replacement process proceeded by a second mechanism by a solid-state ion exchange mechanism even under hydrothermal conditions (Yoshino et. al., 1985).

Recently, a better approach conducted to elucidate the source of the conversion $M^{2+}SO_4$ to $M^{2+}CO_3$, M= Sr or Ba; was proposed based on the crystalline structural differences associated to the physical bulk molar volume change, which also must occur due to the replacement of a large anion SO_4^{2-} by a smaller one CO_3^{2-}. Thus, the study was conducted in large single crystals of celestite $SrSO_4$ and barite $BaCO_3$, which were treated under alkaline hydrothermal conditions using high concentrated carbonated solutions of Na_2CO_3 and K_2CO_3. The mineral celestite single crystals ($SrSO_4$, square plates 10 mm wide and 3 mm thick) were topotaxially converted to strontianite ($SrCO_3$) under alkaline hydrothermal conditions. The reaction was completed in a short reaction time (such as 24 h) at a temperature of 250 ˚C. Increasing the treatment temperature and the molar ratio CO_3^{2-}/SO_4^{2-} accelerated the exchange of SO_4^{2-} with CO_3^{2-} ions. Under these conditions the topotaxial hydrothermal conversion to strontianite is carried out with the formation of intermediate CO_3^{2-}-rich solid solutions in the system $SrCO_3$–$SrSO_4$, this is shown in the Figure 15; and these solid solutions were formed by a controlled crystallization process achieved by the cluster dissolution–recrystallization. An anisotropic dissolution gave a characteristic texture in the converted crystals, and the difference on the reactivity of the celestite crystals in Na_2CO_3 and K_2CO_3 solutions resulted in a different texture inside the pseudomorphical converted strontianite crystals (Rendón-Angeles et. al., 2000b).

Despite the aspect of the converted crystals remained without any change after the conversion process (Fig. 15c), the formation of small holes randomly distributed were produced on outside layer produced as a result of the transformed into the MCO_3 phase Figure 16. However, the morphology of these holes underwent a change due to a simultaneous dissolution of the solid product, the recrystallization process of this phase also occurred at the same place where the previous dissolution occurred. One point that must be emphasized is that the two phases are separated by a sharp boundary in texture, as well as composition. From this observation it is clear that the replacement reaction begins from the surface of the mineral that was in contact with the hydrothermal media (Fig. 16a). In addition, the reaction proceeded by the incorporation of the solvent through the inner porosity. The holes form a zig-zag network inside the crystals which allows incorporating fresh solvent media at the reaction front (Suaréz-Orduña et. al., 2004a; Rendón-Angeles et. al., 2008). This reaction is similar to the ionic replacement process that was found for the conversion of chlorapatite and hydroxyapatite single crystals into

fluorapatite single crystals under hydrothermal conditions (Rendón-Angeles et. al., 2000b). In terms of the macroscopic aspects and crystalline structural differences associated with the replacement of a large ion (SO_4^{2-} = 4.32 Å) by a smaller (CO_3^{2-} = 1.55 Å). However, the completely converted MCO_3 crystals are constituted for very tiny crystals randomly oriented which resemble a polycrystalline arrangement on the converted $M^{2+}CO_3$. Thus in this particular case, the conversion process proceeds with the formation of a converted layer that has a peculiar texture (holes, Fig. 16b) and a moving reaction front. Hence, the conversion of the $M^{2+}SO_4$ mineral species into their related carbonated inorganic compounds; is associated to a pseudomorphic replacement process rather than the ion-exchange process. In addition, at the hydrothermal conditions in which the mineral conversion can be achieved, the pseudomorphic replacement process is mainly achieved by a mechanism of coupled bulk dissolution and precipitation. It is well known that this mechanism promotes the formation of a great wide type of inorganic compounds (Putnis, 2002).

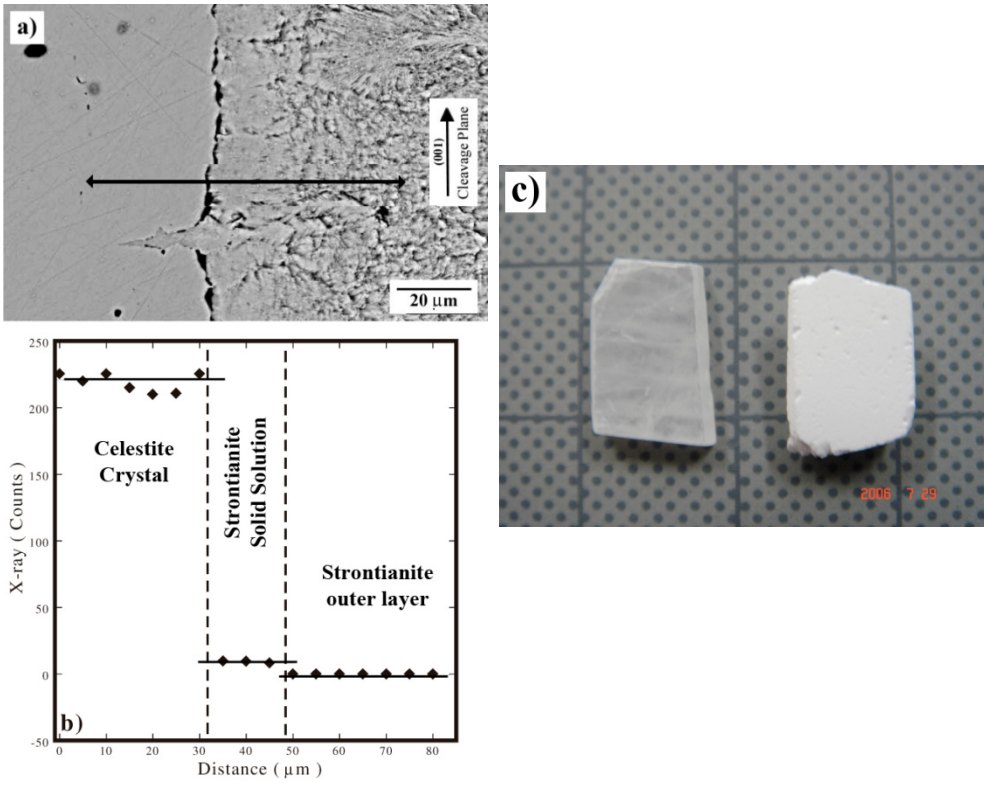

Fig. 15. (a) SEM image of the reaction interface and (b) sulfur concentration in a partially converted celestite crystal obtained by hydrothermal treatment in a Na_2CO_3 solution with a molar ratio CO_3^{2-}/SO_4^{2-} = 10, at 250 ˚C for 1 h. and (c) 96 h, aspects of the original $SrSO_4$ (left) and converted $SrCO_3$ (right). Grid size= 10 mm

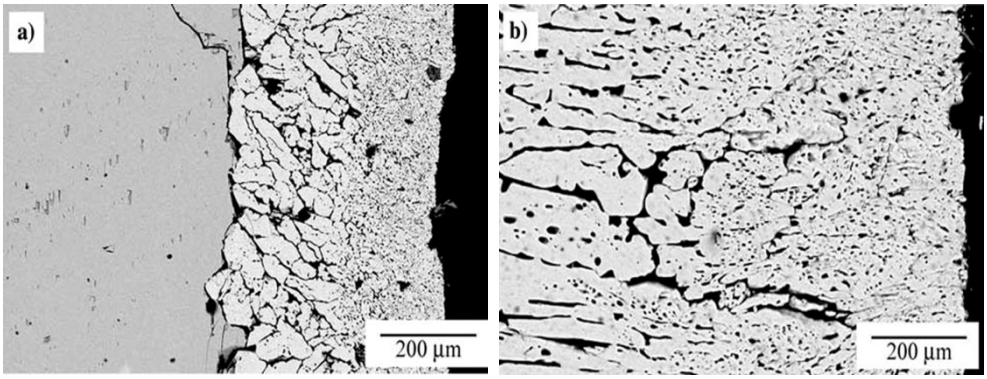

Fig. 16. SEM micrographs of barite crystals converted to barium carbonate after hydrothermal treatment at 250 °C in a Na_2CO_3 solution with a molar ratio CO_3^{2-}/SO_4^{2-} of 10 for different reaction intervals (a) 24 h (b) 192 h (Rendón-Angeles et. al., 2008).

2.5.2 Aspects associated with the formation and control of the residual porosity during the replacement reaction of mineral sulphate species

In terms of the porosity resulted as consequence of the crystalline transformation, this factor has also been the subject of controversy, because the causes that promote its formation are not clarified yet. However, we have recently found that the formation of the residual porosity depends strongly of two principal factors: i) the differences on the molar volume associated with the crystalline structural differences and ii) the chemical stability (solubility) of the new converted crystalline phase in the hydrothermal media. These inferences were established on partially and completely converted $SrCO_3$ specimens obtained by hydrothermal treatments at 250 ^oC for a interval of 24 h with a molar ratio CO_3^{2-}/SO_4^{2-} = 10. The inner volume on the converted crystals was determined by helium picnometry measurements and those results are giving in Figure 17. It is clear that the volume measurements conducted on the completed converted $SrCO_3$ plates at 250 °C for 96 h, revealed that the residual inner porosity value obtained on the specimens treated in Na_2CO_3 solutions is nearly similar to the theoretical value (dotted line in Fig. 17), this value (15.62 %) associated with the reduction of the molar volume, was calculated by considering the unit cell volume values of the parent (celestite, 307.06 $Å^3$) and the product (strontianite, 259.07 $Å^3$). This crystalline structural variation is related with the formation of the residual inner porosity, because macroscopically the crystal plate remains without any change regarding its shape and dimension, therefore, the bulk molar volume reduction does not proceed on the crystal plate and this must be compensated by which is like to proceed the residual porosity. Moreover, the control of the porosity depends on the chemical stability of the phase crystallized with the ion exchange media, once the replacement reaction was completed (Suaréz-Orduña et. al., 2004b). This inference is supported by the fact that when the conversion was carried out in K_2CO_3 solutions, the residual inner porosity on the completed converted $SrCO_3$ plate was markedly increased due to a further dissolution of the converted $SrCO_3$ crystal, in comparison with the porosity obtained the $SrCO_3$ plates transformed with highly concentrated Na_2CO_3 solutions at $CO_3^{2-}/SO_4^{2-} > 5$.

On the other hand, the remaining porosity is limited by the differences on the crystalline structure between the parent and the product. This is likely to occur when a large one replaces a small anion and a change on the structural structure also proceeds. One example was found in the case of the conversion of celestite to $SrCrO_4$, this reaction proceeds at low temperatures (200 °C) in relatively alkaline hydrothermal conditions (K_2CrO_4 solution), with the formation of a peculiar phase on the surface of the partially converted crystals. It is well known that dissolution of mineral species in hydrothermal fluids normally proceeds anisotropically, producing a peculiar texture with holes inside the recrystallized mineral specie (Suaréz-Orduña et. al., 2004a; Rendón-Angeles et. al., 2008). The holes might not be inherited from etch pits produced during the dissolution process, because they did not penetrate the crystals. The factor that has a marked influence in limiting the formation of a residual porosity is related with the replacement of SO_4^{2-} ions by CrO_4^{2-} ions in the $SrSO_4$ crystals. This fact is suggested from the structural change of the orthorhombic to monoclinic structure, which occurs during the conversion. In terms of the global unit cell volume, an expansion process is likely to proceed, therefore, in accordance with the differences on the unit cell volume between that for celestite (312.37 Å^3) and that of $SrCrO_4$ (354.11 Å^3), a volume increase of 41.74 Å^3 is attained in the converted new layer of $SrCrO_4$ as is seen in Figure 18. Hence, the global volumetric unit cell expansion must be compensated by the formation of a continuous solid phase and the formation of some microcracks in this new phase (Rendón-Angeles et. al., 2000b). The formation of a solid phase covering the partially reacted $SrSO_4$ might reduce the transfer of fresh ion exchange media, because under hydrothermal conditions the absence of a texture (small porosity) in the converted phase avoids the penetration of the hydrothermal fluid, coming to an abrupt halt of the replacement reaction

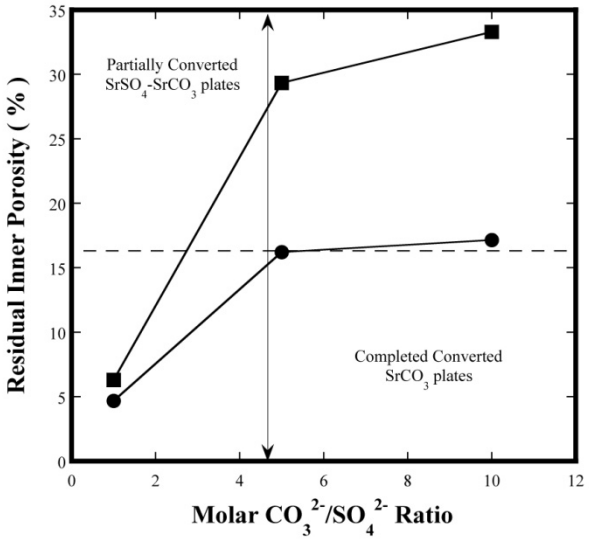

Fig. 17. Variation of the residual porosity on partial and completely converted $SrCO_3$ crystal plates, under hydrothermal conditions at 250 °C for 96 h in (●) Na_2CO_3 and (■) K_2CO_3 solutions with different molar CO_3^{2-}/SO_4^{2-} ratios. Dotted line= theoretical value calculated from the variation of the cell unit lattice associated with the structural conversion.

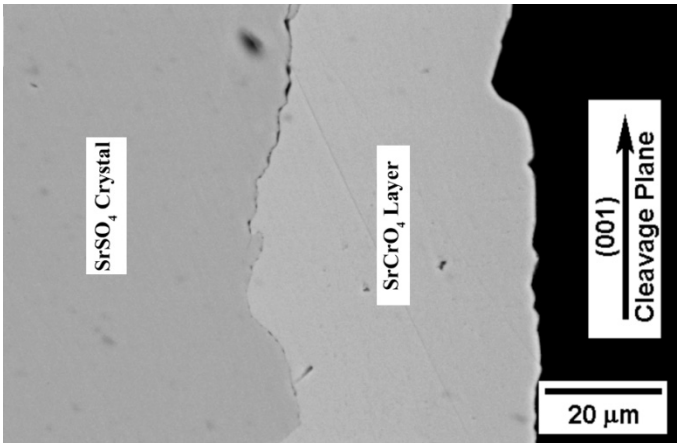

Fig. 18. Partially reacted $SrSO_4$ crystal at 200 °C for 96 h in a hydrothermal media with a molar ratio $CrO_4^{2-}/SO_4^{2-}=1$.

3. Conclusions

The hydrothermal crystallization of advanced materials is an important branch of chemical science and technology, this process has advantages over conventional technologies, namely the purity of products, quality, and performance, and can be consider as a green chemistry process because is environmentally friendly, because reactions consume lesser energy and these can be carried out under controlled parameters in a closed system. Although, the study of a wide number of oxides have provided physico-chemical experimental information related to solid-aqueous interactions, that affect the dissolution-precipitation mechanism main driving force for achieving bulk solid crystallization, coupled with thermodynamic modelling analysis; have contributed to establish the optimum hydrothermal processing conditions that favours the crystallization proceeds at high yield rates. However, still crystallization research work to carry out on those solid-aqueous systems associated to a specific compound that departs from the thermodynamic modelling limits. In addition, the employment of mineral ore as reactant precursors emerges as an interesting route to explore in order to produce other advanced ceramic compounds via the hydrothermal crystallization. Among the new research routes explored for hydrothermal processing, the ionic replacement is able to become common knowledge in the near future as alternative processing route, because this reaction promotes a peculiar microstructure in the transformed material that preserves the bulk original geometrical aspects during a single step hydrothermal crystallization reaction. This processing route can lead to prepare pore net-shaped materials with controlled porosity, which depending on their functional properties of the compound, can be used as gas sensor, substrates for porous catalytic materials, filters, and other applications. The conversion process focused toward a particular preparation of a functional inorganic compound from the mineral transformation requires a proper appreciation of the physico-chemical aspects involved for the solid solution-aqueous solution system. Likewise, to evaluate the likely porosity development in any mineral replacement reaction requires knowledge of the coexisting solid and fluid phases involved and their relative solubility.

4. Acknowledgment

One of the authors JCRA wish to acknowledge CONACYT and COECYT for the financial support trough research grants (Project 34830-U) and (FOMIX-COAH 2003-C02-02), respectively. JCRA and ZMV are indebt to the SNI for the financial support. Many thanks are particularly offered to former Ph D. students that collaborate with the experimental work, Roberto Suarez-Orduña, Laura Patricia Vazquez-Rivas and Yadira Marlen Rangel-Hernandez, also to technicians MSc. Martha Rivas-Aguilar and Eng. Felipe de Jesus Márquez-Torres, whom helped in the preparation of samples and its observation by SEM.

5. References

Bilger, S.; Blab, G. & Förthmann, R. (1997). Sol-gel Synthesis of Lanthanum Chromite Powder, *Journal of the European Ceramic Society*, Vol. 17, No. 8, pp. 1027-1031, ISSN 0955-2219

Byrappa, K. & Yoshimura, M. (2001). *Handbook of Hydrothermal Technology,* William Andrew Publishing/Noyes, ISBN 0-8155-1445-X, New York, USA

Byrappa, K. (2005). *Hydrothermal Processing,* Kirk-Othmer Encyclopedia of Chemical Technology, pp. Copyright John Wiley & Sons, Inc., ISBN 9780471238966

Chakraborty, A.; Basu, R. N. & Maiti, H. S. (2000). Low Temperature Sintering of La(Ca)CrO_3 Prepared by an Autoignition Process, *Materials Letters*, Vol. 45, No. 3-4, (September 2000), pp. 162-166, ISSN 0167-577X

Chen, C. W.; Riman, R. E; TenHuisenb, K. S. & Brown. (2004). Mechanochemical–Hydrothermal Synthesis of Hydroxyapatite from Nonionic Surfactant Emulsion Precursors, *Journal of Crystal Growth*, Vol. 270, pp. 615–623, ISSN 0022-0248

Eckert J. O.; Hung-Houston, C. C.; Gersten, B. L.; Lencka, M. M. & Riman, R. E. (1996). Kinetics and Mechanism of Hydrothermal Synthesis of Barium Titanate, *Journal of the American Ceramic Society* Vol. 79, No. 11, (November 1996), pp. 2929-2939, ISSN 0002-7820

Gersten, B. l.; Lencka, M. M. & Riman R. E. (2004). Low Temperature Hydrothermal Synthesis of Phase-Pure (Br,Sr)TiO_3 Perovskite Using EDTA, *Journal of the American Ceramic Society*, Vol. 87, No. 11, (January 2004), pp. 2025-2032, ISSN 0002-7820

Hessien, M. M.; Hassan, M. M. & El-Barawy, K. (2009). Synthesis and Magnetic Properties of Strontium Hexaferrite from Celestite Ore, *Journal of Alloys and Compounds*, Vol. 476, No. 1-2, 12 (May 2009), pp. 373-378, ISSN 0925-8388

Ianculescu, A.; Braileanu, A.; Pasuk, I. & Zaharescu, M. (2001). Phase Formation Study of Alkaline Earth-doped Lanthanum Chromites, *J. Therm. Anal. Calorim.,* Vol. 66, No. 2, (November 2001), pp. 501-507, ISSN: 1388-6150

Inagaki, M.; Yamamoto, O. & Hirohara, M., (1990). Synthesis of $LaCrO_3$ from Complex Precipitation and its Electrical Conductivity, *Journal of the Ceramic Society of Japan*, Vol. 98, pp. 675–678, ISSN 1882-0743

Kashkurov, K. F., Nikitichev, P. I., Osipov, V. V., Sizova, L. D., & Simonov, A. V. (1968). Growth of Large Corundum Crystals by the Hydrothermal Method, *Soviet Physics Crystallografia*, Vol. 12, pp. 837– 839, ISSN 0038-5638

Kobe K. A. & Deiglmeier N. J. (1943). Strontium Carbonate, Conversion from Strontium Sulfate by Metathesis with Alkali Carbonate Solution, *Industrial and Engineering Chemistry*, Vol. 35, No. 3, pp. 323-325, ISSN 1226-086X

Komarneni S., Roy R. & Li, Q. H. (1992). Microwave-Hydrothermal Synthesis of Ceramic Powders, *Materials Research Bulletin*, Vol. 27, pp. 1393-1405, ISSN 0025-5408

Komarneni, S. ; Komarneni Y. S.; Newalkar, B.; Stour, S. (2002). Microwave-Hydrothermal Synthesis of Al-Sustituted Tobermorite from Zeolites. *Materials Research Bulletin,* Vol. 3, (March 2002), pp. 1025-1032, ISSN 0025-5408

Kubo, T.; Hogiri, M.; Kagata, H. & Nakahira, A. (2009). Synthesis of Nano-Sized $BaTiO_3$ Powders by The Rotatory-Hydrothermal Process, *Journal of the American Ceramic Society*, Vol. 92, No. S1, (January 2009), pp. S172-S176, ISSN 0002-7820

Lee, S. K.; Choi, G.J.; Hwang, U. Y.; Koo, K. K. & Park, T. J. (2003). Effect of Molar Ratio of KOH to Ti-Isopropoxide on the Formation of $BaTiO_3$ Powders by Hydrothermal Method, *Materials Letters*, Vol. 57, No. 15, (April 2003), pp. 2201-2207, ISSN 0167-577X

Lencka, M. M. & Riman, R.E . (1993). Thermodynamic Modeling of Hydrothermal Synthesis of Ceramic Powders, *Chemistry of Materials*, Vol. 5, (October 1993), pp. 61-70, *ISSN* 0897-4756

Lencka, M.M. & Riman, R. E. (1995). Thermodynamics of the Hydrothermal Synthesis of Calcium Titanate with Reference to Other Alkaline-Earth Titanates, *Chemistry of Materials*, Vol. 7, (September 1995), pp. 18-25, *ISSN* 0897-4756

Lencka, M.M. & Riman, R.E. (2002). *Intelligent Systems of Smart Ceramics*, Encyclopedia of Smart Materials, Vol. 1, John Wiley & Sons, Inc., ISBN 9780-471216278, N.J, USA

Marchisio, D. L. (2009). On the Use of Bi-Variate Population Balance Equations for Modelling Barium Titanate Nanoparticle Precipitation, *Chemical Engineering Science,* Vol. 64, (February 2009), pp. 697-708, ISSN 0009-2509

Moreira, M. L.; Mambrini, G. P.; Volanti, D. P.; Leite, E. R.; Orlandi, M. O.; Pizani, V. R. Mastelaro, P.S.; Paiva-Santos, C. O.; Longo, E. & Varela, J. A. (2008). Hydrothermal Microwave: A New Route to Obtain Photoluminescent Crystalline $BaTiO_3$ Nanoparticles*, Chemistry of Materials*, Vol. 20, pp. 5381–5387*, ISSN* 0897-4756

Moon, J.; Kerchener, J. A.; Krarup, H. & Adair, H. (1999). Hydrothermal Synthesis of Ferroelectric Perovskites from Chemically Modified Titanium Isopropoxide and Acetate Salts, *Journal of Materials Research,* Vol. 14, No. 2, (February 1999), pp. 425-434, ISSN 0884-2914

Oledzka, M.; Lencka, M. M.; Pincelup, M. P.; Mikulka-Bulen, K.; McCandlish, L. & Riman, R. (2003). Influence of Precursor on Microstructure and Phase Composition of Epitaxial Hydrothermal $PbZr_{0.7}Ti_{0.3}O_3$ Films, *Chemistry of Materials,* Vol. 15, (March 2003), pp. 1090-1098, ISSN 0897-4756

Peterson, C. R. & Slamovich, E. B. (1999). Effect of Processing Parameters on the Morphology of Hydrothermally Derived $PbTiO_3$ Powders, *Journal of the American Ceramic Society*, Vol. 82, No. 7, (July1999), pp. 1702-1710, ISSN 0002-7820

Putnis, A. (2002). Mineral Replacement Reactions: From Macroscopic Observations to Microscopic Mechanisms, *Mineral Magazine*, Vol. 66, No.5, (October 2002), pp. 689-708, ISSN 0026-461X

Putnis A. (2009). Replacement Reactions, *Review Mineral Geochemistry*, Vol. 70, pp. 87-124, ISSN 1529-6466

Qi, L.; Lee, B. I.; Badheka, P.; Yoon, D. H.; Samuels, W. D. & Exarhos, G. J., (2004). Short-range Dissolution–Precipitation Crystallization of Hydrothermal Barium Titanate, *Journal of the European Ceramic Society*, Vol. 24, No. 13, (October 2004), pp. 3553–3557, ISSN 0955-2219

Ramkrishna, D. & Mahoney, A. W. (2002) Population Balance Modeling Promise for the Future, *Chemical Engineering Science*, Vol. 57, (February 2002), pp. 595 – 606, ISSN 0009-2509

Rangel-Hernandez, Y. M.; Rendón-Angeles, J. C.; Matamoros-Veloza, Z.; Pech-Canul, M. I.; Diaz-de la Torre, S. & Yanagisawa, K. (2009). One-step Synthesis of Fine $SrTiO_3$ Particles Using $SrSO_4$ Ore Under Alkaline Hydrothermal Conditions, *Chemical Engineering Journal*, Vol. 155, No. 2, (January 2009), pp. 483–492, ISSN 1385-8947

Riman R.E .; Suchanek, W. L. & Lencka, M. M. (2002). Hydrothermal Crystallization of Ceramics, *Annales de Chimie Science des Materiaux*, Vol. 27, No. 6, (November 2002), pp. 15-36, ISSN 0151-9107

Rivas-Vázquez, L. P.; Rendón-Angeles, J. C.; Rodríguez-Galicia, J. L.; Zhu, K. & Yanagisawa, K. (2004). Hydrothermal Synthesis and Sintering of Lanthanum Chromite Powders Doped With Calcium, *Solid State Ionics*, Vol. 172, No. 1-4, (August 2004), pp. 597-600, ISSN 0167-2738

Rivas-Vázquez, L. P.; Rendón-Angeles, J. C.; Rodríguez-Galicia, J. L.; Gutiérrez-Chavarria, C. A.; Zhu, K. & Yanagisawa, K. (2006). Preparation of Calcium Doped $LaCrO_3$ Fine Powders by Hydrothermal Method and its Sintering, *Journal of the European Ceramic Society*, Vol. 26, No. 1-2, (October 2006), pp. 81-88, ISSN 0955-2219

Rendón-Angeles, J. C.; Yanagisawa, K.; Ishizawa, N. and Oishi, S. (2000a). Effect of Metal Ions of Chlorapatites on the Topotaxial Replacement by Hydroxyapatite under Hydrothermal Conditions, *Journal of Solid State Chemistry*, Vol. 154, No. 2, (November 2000), pp. 569-578, ISSN 0022-4596

Rendón-Angeles, J. C.; Yanagisawa, K.; Ishizawa, N. and Oishi, S. (2000b). Topotaxial Conversion of Chlorapatite and Hydroxyapatite to Fluorapatite by Hydrothermal Ion Exchange, *Chemistry of Materials* Vol. 12, No. 8, pp. 2143-2150, (June 2000), *ISSN* 0897-4756

Rendón-Angeles, J. C.; Pech-Canul, M. I.; López-Cuevas, J.; Matamoros-Veloza, Z. & Yanagisawa., K. (2006). Differences on the Conversion of Celestite in Solutions Bearing Monovalent Ions Under Hydrothermal Conditions, *Journal of Solid State Chemistry*, Vol. 179, No. 12, (December 2006), pp. 3645-3652, ISSN 0022-4596

Rendón-Angeles, J. C.; Matamoros-Veloza, Z.; López-Cuevas J.; Pech-Canul, M. I & Yanagisawa, K. (2008). Stability and Direct Conversion of Mineral Barite Crystals in Carbonated Hydrothermal Fluids, *Journal of Material Science*, Vol. 43, pp. 2189, ISSN 0022-2461

Rendón-Angeles, J. C., Yanagisawa, K.; Matamoros-Veloza, Z.; Pech-Canul, M. I.; Mendez-Nonell, J. & Diaz-de la Torre, S. (2010). Hydrothermal Synthesis of Perovskite Strontium Doped Lanthanum Chromite Fine Powders and its Sintering, *Journal of Alloys and Compounds*, Vol. 504, No. 1, (August 2010), pp. 251-256, ISSN 0925-8388

Roy, R. (1994). Accelerating the Kinetics of Low-Temperature Inorganic Syntheses, *Journal of Solid State Chemistry,* Vol. 111, (July 1994), pp. 11-17, ISSN 0022-4596

Schubert, U. and Hüsing, N., 2000. Synthesis of Inorganic Materials

Shi, S. &. Hwang, J. Y. (2003). Microwave-Assisted Wet Chemical Synthesis: Advantages, Significance, and Steps to Industrialization, *Journal of Mineral & Materials & Characterization & Engineering*, Vol. 2, No.2, pp. 101-110, ISSN: 1539-2511

Suárez-Orduña, R; Rendón-Angeles, J. C.; López-Cuevas, J; & Yanagisawa, K. (2004a). The Conversion of Mineral Celestite to Strontianite Under Alkaline Hydrothermal

Conditions, *Journal of Physics: Condensed Matter*, Vol. 16, pp. S1331-S1344, ISSN 0953-8984

Suárez-Orduña, R.; Rendón-Angeles, J. C.; Matamoros-Veloza, Z. & Yanagisawa, K. (2004b). Exchange of SO_4^{2-} Ions With F^- Ions In Mineral Celestite Under Hydrothermal Conditions, *Solid State Ionics,* Vol. 172, pp. 393-393, ISSN 0167-2738

Suchanek, W. L.; Shuka, P.; Byrappa, K.; Riman, R. E.; TenHuisen, K. S. & Janas, V. F. (2002). Mechanochemical–hydrothermal synthesis of Carbonated Apatite Powders at Room Temperature, *Biomaterials*, Vol. 23, (April 2001), pp. 699–710, ISSN 0142-9612

Suchanek, W. L.; Lencka M. M; & Riman, R. E. (2004). Hydrothermal Synthesis of Ceramics Materials, *Aqueous System at Elevated Temperature and Pressure Physical Chemistry in Water, Steam and Hydrothermal Solutions*, Chapter 18, ISBN 0-12-544461-3, Elsevier Ltd., New Jersey, USA

Shi, S. &. Hwang, J. Y. (2003). Microwave-Assisted Wet Chemical Synthesis: Advantages, Significance, and Steps to Industrialization, *Journal of Mineral & Materials & Characterization & Engineering*, Vol. 2, No.2, pp. 101-110, ISSN 1539-2511

Spooren, J.; Rumplecker, A.; Millange, F. & Walton, R. I. (2003). Subcritical Hydrothermal Synthesis of Perovskite Manganites: A Direct and Rapid Route to Complex Transition-Metal Oxides*, Chemistry of Materials* Vol. 15, (March 2003), pp. 1401–1403, ISNN 0897-4756

Testino, A.; Buscaglia, V.; Buscaglia, M. T.; Viviani, M. & Nanni, P. (2005). Kinetic Modeling of Aqueous and Hydrothermal Synthesis of Barium Titanate ($BaTiO_3$), *Chemistry of Materials*, Vol. 17, (September 2005), pp. 5346-5356*, ISSN* 0897-4756

Tiwary, R. K.; Narayan, S. P. & Pandey, O.P. (2008). Preparation of Strontium Hexaferrite Magnets from Celestite and Blue Dust by Mechanochemical Route, *Journal of Mining and Metallurgy, Section B*, Vol. 44, (February 2008), pp. 91 - 100, ISSN 1450-5339

Vivekanandan, R. & Kutty, T. R. N. (1989). Characterization of Barium Titanate Fine Powders Formed From Hydrothermal Crystallization, *Powder Technology*, Vol. 57, No. 3, (March 1989), pp. 181 – 192, ISSN 1570-1468

Wada, S. Suzuki T. & Noma T. (1995). Preparation of Barium Titanate Particles by Hydrothermal Method and Their Characterization, *Journal of the Ceramic Society of Japan*, Vol. 103, No. 12, (December 1995) pp. 1220-1227, ISSN 1882-0743

Walton, R. I.; Millange, F. Dmith, R. I., Hansen, T. C. & O'hare, D. (2001). Real Time Observation of the Hydrothermal Crystallization of Barium Titanate Using In Situ Neutron Powder Difracction. *Journal of the American Chemical Society*, Vol. 123, pp. 12547-12555, ISSN 0002-7863

Wang, Y.; Xu, G.; Yang, L.; Ren, Z.; Wei, X.; Weng, W.; Du, P.; Shen, G. & Han, G. (2009). Formation of Single-Crystal $SrTiO_3$ Dendritic Nanostructures via a Simple Hydrothermal Method, *Journal of Crystal Growth*, Vol. 311, No. 8, (April 2009), pp. 2519-2523, ISSN 0022-0248

Wei, X.; Xu, G.; Ren, Z.; Xu, C.; Sheng, G. & Han, G. (2008). PVA-Assited Hydrothermal Sinthesis of $SrTiO_3$ Nanoparticles with Enhanced Photocatalytic Activity for Degradation of RhB, *Journal of the American Ceramic Society*, Vol. 91, No. 11, (November 2008), pp. 11-17, ISSN 0002-7820

Wendelbo, R.; Akporiaye, D. E.; Karlsson, A.; Plassen, M. & Olafsen, A. (2006). Combinatorial Hydrothermal Synthesis and Characterization of Perovskites, *Journal of the European Ceramic Society,* Vol. 26, No. 6, pp. 849-859, ISSN 0955-2219

Yanagisawa, K.; Rendón-Angeles, J. C.; Kanai H. & Yamashita, Y. (1999). Stability and Single Crystal Growth of Dielectric Materials Containing Lead Under Hydrothermal Conditions, *Journal of the European Ceramic Society*, Vol. 19, No. 6-7, (June 1999), pp. 1033-1036, ISSN 0955-2219

Yoshimura, M. & Suchanek, W. (1997). In Situ Fabrication of Morphology-Controlled Advanced Ceramic Materials by Soft Solution Processing, *Solid State Ionics*, Vol. 98, No. 3-4, (June 1997) pp. 197–208, ISSN 0167-2738

Yoshino, K.; Nishino, T.; Yoshino, M. & Yoshimura, S. (1985). Exchange Reaction between Alkaline Earth Carbonate and Sulfate under Hydrothermal Condition, *Yogyo-Kyokai-Shi*, Vol. 93, No. 6, pp. 334-337, ISSN 0372-7718

Zhang, S.; Han, Y.; Chen, B. & Song, X. (2001). The Influence of $TiO_2 \bullet H_2O$ Gel on Hydrothermal Synthesis of $SrTiO_3$ Powders, *Materials Letters*, Vol. 51, No. 4, (November 2001), pp. 368-370, ISSN 0167-577X

Zhang, S.; Liu, J.; Han, Y.; Chen, B. & Li, X. (2004). Formation Mechanisms of $SrTiO_3$ Nanoparticles Under Hydrothermal Synthesis, *Materials Science and Engineering B,* Vol. 110, No. 1, (June 2004), pp. 11-17, ISSN 0921-5107

Zheng, W.; Pang, W.; Meng, G. & Peng, D. (1999). Hydrothermal Synthesis and Characterization of $LaCrO_3$, *Journal of Materials Chemistry*, Vol. 9, pp. 2833–2836, ISNN 0959-9428